Factors influencing aerosol and precipitation ion chemistry in urban background of Moscow megacity

Factors influencing aerosol and precipitation ion chemistry in urban background of Moscow megacity

Alessandro Zappi[1], Olga Popovicheva[2], Laura Tositti[1], Marina Chichaeva[3], Irina Eremina[3], Anne Kasper-Giebl[4], Ying Tsai[5], Dmitry Vlasov[3], Nikolay Kasimov[3]

[1] Department of Chemistry "Giacomo Ciamician", University of Bologna, Bologna, Italy

[2] SINP, Lomonosov Moscow State University, Moscow, Russia

[3] Faculty of Geography, Lomonosov Moscow State University, Moscow, Russia

[4] Institute of Chemical Technologies and Analytics, TU Wien, Vienna, Austria

[5] Department of Environmental Engineering and Science, Chia Nan University of Pharmacy and Science, Tainan 71710, Taiwan

Corresponding authors:

Olga Popovicheva: olga.popovicheva@gmail.com

Lomonosov Moscow State University, Leninskie Gory, 1, 199991, Moscow, Russia

Tel: +7 939 49 54

Laura Tositti: laura.tositti@unibo.it

Via Selmi 2, 40126, Bologna, Italy

Tel: +39 051 2099488

Fax: +39 051 2099456

ABSTRACT

In-depth study of aerosol and precipitation ion chemistry was carried out in order to cover an existing data gap in the seasonal-dependent ionic data in Moscow urban background atmosphere. Literature about atmospheric pollution in this megacity is, indeed, still poor, despite its peculiar climatological characteristics that make it a very interesting site for atmospheric research. Particulate matter (PM) and precipitation were collected at Moscow urban background during spring of 2018, summer, and autumn of 2019. Aerosol inorganic ions are characterized for the whole period, carboxylic acids and sugars for summer. Inorganic ions constitute a major PM_{10} fraction of 27% in autumn, it drops down to 16.5% in summer. Dominance of secondary inorganic aerosol (SIA) over all the other inorganic ion species is determined. Na^+ and Ca^{2+} shows the largest variability between seasons, with maximum in summer and spring, respectively. Excess of anions in autumn is indicated by ion balance while adding carbonates, spring and summer aerosol is found electroneutral. Chloride depletion phenomenon follows the snow melt and remobilization of salt applied to roads for deicing, demonstrating the biggest impact in summer. Degree of neutralization of ammonia as sulfate and nitrate is found by the correlation between the concentration of NH_4^+ and calculated from SO_4^{2-} and NO_3^-. Inorganic fraction in PM_{10} is higher (16.5%) than total carboxylic acids (3.5%), and total sugars and anhydrosugars (0.8%). Concentration polar plots show ion variation jointly with wind speed and wind direction and the source origin. Highest SIA concentrations relate a cluster of the prevalent air mass transportation and indicate the source in the northwestern direction in spring and summer. K^+ acts as a marker of fires in spring and summer as well as of the domestic biomass burning in the region around a megacity in autumn. Source apportionment of inorganic ion and BC by Varimax analysis reveals major sources namely SIA, soil resuspension, biomass burning, deicing salt, and fossil fuel combustion. In summer, organic ions, anhydrosugars, and sugars shows additional impact of photochemistry and biological activities. Rainfall is heavier in summer than in autumn, with pH of acid rain during spring and summer. The highest concentrations for almost all ions were observed in spring, except HCO_3^-. Precipitation composition is described with aerosol wet removal by seasonal variability of SIA scavenging factors, decreasing in summer and increasing in autumn and spring.

Keywords: Moscow; air pollution; rain pollution; Varimax; aerosol ion chemistry

1. Introduction

Airborne particulate matter (PM) is one of the atmospheric pollutants of major concern associated not only to major air quality issues in connection with adverse effects on health (WHO, 2013) and the environment, but also with climate change (Fuzzi et al., 2015). PM is a multiphase system including a large number of components, of both primary and secondary origin, and in most cases prone to further physicochemical modifications (Pöschl and Shiraiwa, 2015; Pöschl, 2005; Raes et al., 2000). Owing to the recognized importance of this complex pollutant, great efforts have been applied worldwide in order to monitor and characterize it as well as to fix thresholds and regulations, allowing to prevent or limit adverse effects on human health and environment. The understanding of the processes leading to PM formation and origin requires to associate them to source profiling and quantification. For these reasons PM chemical speciation is of utmost importance since it allows to identify harmful substances as well as sources, providing tools for mitigation and prevention of potential hazards.

The major components of PM are elemental and organic carbon, sea salt, crustal materials from soil/road dust, and water soluble species (ammonium, sulfate, and nitrate) known as Secondary Inorganic Aerosol (SIA) (Seinfeld and Pandis, 2016). Among the PM components, ions play a major role both because of their abundance and massive contribution to aerosol mass load. Each ion determined is associated to specific sources of emission and formation pathways (Raes et al., 2000). Due to their water-soluble nature, ions also affect the acidity of precipitation. They are a key in precipitation formation processes, thus contributing to the hydrological cycle (Reiss et al., 2007; Weber et al., 2016; Dadashazar et al., 2019).

In European urban areas, ammonium sulfate and nitrate concentrations are abundant (Putaud et al., 2010; Tositti et al., 2014). Dusts (Brattich et al., 2015; Tositti et al., 2021) may contribute to calcium and magnesium, usually in the form of relatively soluble carbonates capable, beside ammonia, to add neutralization potential to acidic species (Morozzi et al., 2021; Tositti et al., 2018a). Coastal areas are affected by sea salt compounds starting from the most abundant, i.e. NaCl, and extending to further saline compounds (Koçak et al., 2007; Lung et al., 2004). In inland cities during the cold period the sources of particulate sodium and chloride are de-icing agents (DIAs) (Kolesar et al., 2018; Kotowski et al., 2020; Stieger et al., 2018; Tositti et al., 2018a).

Ambient organic ions are associated with secondary organic aerosol (SOA), mainly produced by oxidation of volatile organic compounds (VOCs) (Kawamura and Bikkina, 2016; Pavuluri et al., 2010; Yang and Yu, 2008). Though at significantly lower concentration level than SIA, they are present in significant “chemodiversity” (Tositti et al., 2018a). The speciation and profiling of SOA is a very hard and complex task (Gentner et al., 2017; Pio et al., 2005; Schauer et al., 2002; Wang et al.,

2006), owing to a number of precursors and complexity of oxidation patterns. Oxidation, in fact, is carried out by a series of oxidizing species in the troposphere such as OH and NO_3 radicals, group of peroxy-radicals and ozone (Seinfeld and Pandis, 2016).

High polarity of both SIA and SOA is a key in the so-called cloud processing, wherein aerosol particles induce water vapor condensation upon cloud condensation nuclei until water droplets or snow crystals are formed. Precipitation chemistry largely reflects the composition of precursor aerosols (Pruppacher and Klett, 2010) whose degree of neutralization affects precipitation acidity (pH). Acidity of rains constituted an extremely serious environmental problem in Europe which, owing to effective policies of fuel management, led to a substantial solution of acid rain problems from the late 70's to date (Tositti et al., 2018b; Vet et al., 2014; Vuorenmaa et al., 2018).

Factors influencing ion chemistry are more important in the urban environment where exposure and hazard to air pollution are sensibly higher, owing to the significant population density and related activities such as industry, transport, and heating etc. In this respect, megacities such as Moscow with over ten million inhabitants require a special focus, since emissions and consequent air quality standards might reveal even more unsafe for human health, material infrastructures as well as cultural heritage (Baklanov et al., 2016).

Emission sources in Moscow as a high latitude megacity have several specific features. Centralized heating supply is seasonally operated from the end of September until the beginning of May. Moscow power and heating plants are almost totally supplied with natural gas. Biomass and coal are not used either for industrial, domestic heating, or individual purposes, differently from many European and Asian cities (Diapouli et al., 2017; Nava et al., 2015). Biomass burning (BB) is not recognized by the local Environmental Agency as a significant source of aerosol pollution in Moscow (Kul'bachevskii, 2021). However, largely populated region in the city outskirts (Moscovskaya Oblast) applies biomass for many scopes, such as wood burning for domestic stoves, agricultural cleaning work, and summer recreational activities, that should be considered for air quality assessment. Seasonal light absorption measurements supported the assessment for the BB contribution in the region around Moscow in autumn and winter (Popovicheva et al., 2022). Moreover, combined organic and statistical analysis differentiated the impact of agriculture fires in spring (Popovicheva et al., 2020b).

Differently from the rest of Europe (Finardi et al., 2014; Font et al., 2019; Tang et al., 2014), the knowledge of Moscow megacity aerosol and its sources is limited. Black carbon (BC) pollution in the Moscow urban background (Popovicheva et al., 2020a) as well as in the Moscow center (Golitsyn et al., 2015) indicated a strong impact of transport. The first comprehensive aerosol characterization in the urban background of Moscow megacity included ions in spring only (Popovicheva et al., 2020c). BB markers (levoglucosan and K^+ ions) proved the impact of wildfires during the extreme

smoke event in August of 2010 (Popovicheva et al., 2014) and agricultural fires (Popovicheva et al., 2020c).

Annual records of precipitation in 2012 in Moscow showed the significant increase of its acidity due to the presence of deicing salts (Eremina et al., 2015). The total ionic composition in rains did not change in the last years, while chloride and sodium concentrations were increased. Such finding was associated with DIAs, abundant due to the winter road management in Moscow (Eremina et al., 2015). Despite long-term statistical data for rain acidity and composition (Chubarova et al., 2014), a limited knowledge about factors influencing both particulate and precipitation ions chemistry is available to date for Moscow environment. This situation is further deteriorated by the fact that the Environmental Protection Agency "Mosecomonitoring" conducts the measurements for only PM_{10} and $PM_{2.5}$ mass concentrations at some monitoring stations, without any PM speciation.

This paper therefore aims to cover an existing data gap for the aerosol and precipitation ion chemistry in Moscow urban background. We present the results for the seasonal variation of ionic composition obtained in a sampling campaign carried out in periods of spring 2018, summer and autumn 2019. Descriptive statistics are used to provide PM_{10} and ion seasonal characteristics as well as the comparison between Moscow and some large cities. Constraints of aerosol electroneutrality highlights the ion chemistry of neutralizing agents such as ammonia and carbonates. Varimax and correlation analyses trace the main sources of aerosol and rain ionic species. Black carbon and levoglucosan are considered together with ionic species for improved source apportionment in summer. The relevance of the aerosol chemical speciation to meteorological parameters and air mass transportation are investigated by using the both the conditional probability function (CPF) based on the bivariate polar plot and the Lagrangian integrated trajectory (HYSPLIT) model with the cluster analyses.

2. Materials and methods

2.1 Study Area

Moscow metropolitan area (55° 45' N; 37° 37' E at the city center; mean altitude 150 m a.sl.) is located in the center of the European part of Russia (map in Fig.1). Moscow covers an area of 2561 km^2 and has a registered population exceeding 12.5 million, which makes it one of the most densely populated northernmost megacities in Europe. Moscow is characterized by a humid continental climate (Dfb according Köppen climate classification) with ~685 mm precipitation per year (Chubarova et al., 2014) which are represented by snow for about one third of year (mainly from late October to March), and by rain for the other part of the year with a maximum rainfall amount in summer (on average ~61 mm in June). According to the record of the Meteorological Observatory (MO) MSU over the 60-year period (1954–2013) (Chubarova et al., 2014), significant warming of regional climate with a positive temperature trend of 0.07°C/year is observed. Southwestern wind (5-10 m s^{-1}) prevails during all seasons (https://weatherspark.com). Highest wind speeds are typical of fall and winter. Clean Arctic air masses transported from the North are recorded especially in winter while aged plumes from agriculture and wildfires pollute the Moscow atmosphere in spring and summer. Moderate average air temperatures, low solar UV radiation levels, and good ventilation make the accumulation of primary emitted pollutants and the photochemical formation of secondary pollutants less intensive in Moscow (Elansky et al., 2018). Operation of centralized heating system begins and ends in Moscow when the temperature decreases below 8°C and increases above 8°C, respectively. Thus, the heating period divides the whole year formally on cold and warm with respect to its operation.

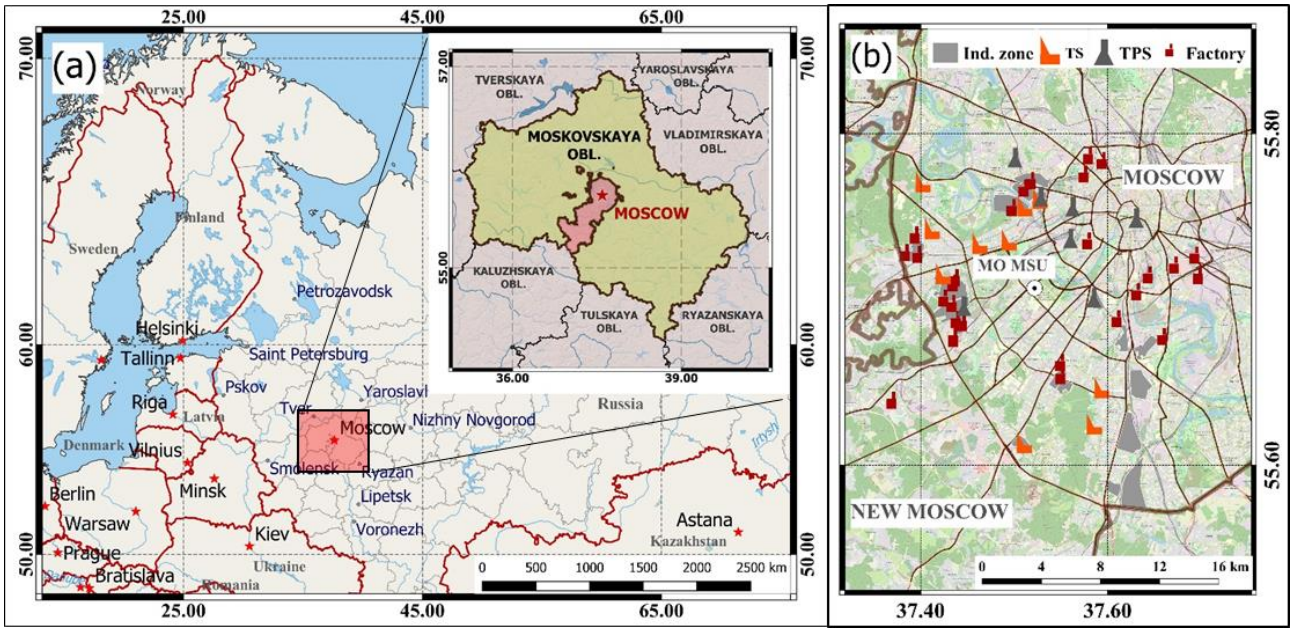

Figure 1. a) Location of Moscow megacity in European part of Russia. Insert is Moscow and Moscovskaya Oblast nearby. b) Southwest sector of Moscow area including New Moscow. Location of sampling site at Meteorological Observatory of Moscow State University (MO MSU) (55° 42' N;

37° 31’ E) is indicated. Industrial zones (Ind.zone), thermal power stations (TPS), thermal stations (TS), and factories in the southwest sector of Moscow are indicated.

According to air quality characterization, Moscow is classified among the slightly polluted megacities in Europe and North America (Elansky et al., 2018). Traffic exhaust constitutes 93% of the overall gaseous megacity emissions (Bityukova and Mozgunov, 2019). While automobilization is growing in Moscow, intensive implementation of higher ecological classes of engines, a declining share of trucks and better quality of fuel promote the improvement of vehicle ecological parameters. Assuming that currently in Moscow the vehicles are powered with desulphurized fuels, traffic is no longer a significant source of SO_2. However, high concentrations of NO_x and CO are still an issue (Elansky et al., 2014), with the potential contributing significantly to SIA by means of active oxidation capacities of the atmosphere (Prinn, 2003; Seinfeld and Pandis, 2016). Around 50% of all pollutant emissions from industrial sources and thermal power stations are emitted by companies producing and redistributing energy, gas, and water. The currently fast urban expansion especially in New Moscow area (Fig.1) additionally contributes to an aerosol buildup in Moscow.

2.2. Aerosol and precipitation sampling

The sampling campaign was conducted at the Aerosol Complex located at Meteorological Observatory of Moscow State University (MO MSU) in the MSU campus, southwest of Moscow city (Fig.1). MO MSU is not directly affected by local pollution sources such as large transport roads or industrial facilities, the residential area and a highway takes place about 800 m south of the observatory, and industrial area is situated at about 3 km. MO MSU site can be therefore classified as an urban background (Chubarova et al., 2014).

Sampling of particulate matter and precipitation was performed during three seasons: spring 2018 (from April 3rd to May 22nd), summer 2019 (from May 29th to July 31st), and autumn 2019 (from September 5th to December 31st). In this work the term “seasons” is used according to the astronomical and not the meteorological convention. PM sampling was not available after December 31st due to the harsh weather conditions which compromised the sampler, preventing the collection of further winter samples. Samples collected in December (11) were merged to the autumn dataset according to the astronomical convention, therefore relating December to autumn as an overall cold season

Particles with a diameter less than or equal to 10 µm (PM_{10}) were daily collected over 24-hour periods from 5 p.m. of a given day to 5 p.m. of the next day. In spring and autumn sampling was performed on 47 mm quartz fiber filters (Pall Science, New York, USA), previously heated at 600^{o}C for 5 h.

Polyethylene terephthalate 47 mm filters (Merck, Germany) were used for summer sampling. An aspirator using a PM_{10} impactor was operated at an air flow of 1 m^3 h^{-1} by, and the pumped volume was reported in standard atmospheric conditions. Totally, 35, 56 and 67 aerosol samples were collected in spring, summer, and autumn, respectively.

Both types of precipitation (rainfall and snow) were collected at a height of 2 m from the ground surface, using a PVC funnel with an exposed area of 1600 cm^2 and a polyethylene vessel as a bulk collector. Totally, 16, 23 and 45 precipitation samples were collected in spring, summer, and autumn, respectively.

Meteorological parameters (temperature, relative humidity, pressure, precipitation, wind speed, and wind direction) were obtained at a 3 h time resolution by the MO MSU meteorological service. PM_{10} mass concentrations were collected using the tapered element oscillating microbalance TEOM 1400a (Thermo Environmental Instruments Inc., Waltham, MA, USA) by Mosecomonitoring (https://mosecom.mos.ru/home-page/). Additionally, continuous aerosol equivalent BC (eBC) concentrations were measured using the custom made portable aethalometer, for more details see elsewhere (Popovicheva et al., 2020a). BC is mainly formed by the incomplete combustion of fossil fuels (diesel, gasoline, gas, coal) in emissions of transport, energy production, residential heating and biomass burning. Therefore, in this study BC is used as a marker of combustion for the source apportionment together with ions. Further in the text we will call eBC as BC according to commonly accepted terminology.

2.3 Analytical Procedures

Aerosol samples were analyzed for water-soluble ionic species, namely cations, including sodium (Na^+), ammonium (NH_4^+), potassium (K^+), magnesium (Mg^{2+}) and calcium (Ca^{2+}), and anions including chloride (Cl^-), nitrate (NO_3^-), and sulphate (SO_4^{2-}), using ion chromatography as described elsewhere (Golobokova et al., 2020; Popovicheva et al., 2020c; Tsai and Kuo, 2013). For the extraction phase, the polyethylene terephthalate filter was placed in 5.0 mL of ultrapure water, then shaken for 90 min and filtered through an ester acetate syringe membrane of pore size 0.2 μm. Quartz filter were extracted with 8 ml ultrapure water in an ultrasonic bath for 30 min, then the solution was filtered through acetate cellulose filters (porosity 0.2 μm). Anions of spring samples were separated by an ion-exchange column (Ion Pac AS17A, Thermo Fisher, USA) in isocratic conditions using 1.8 mM Na_2CO_3 + 1.7 mM $NaHCO_3$, an AMMS suppressor and conductivity detection. Cations were separated on Ion Pac CS12A using 38 mM methane sulfonic acid (MSA), the CSRS suppressor and a conductivity detector. The detection limits varied between 2 and 20 ng m^{-3}, the lowest values were obtained for sodium and chloride.

In summer and autumn samples, inorganic cations were determined using a Dionex ICS-1000 equipped with a gradient pump (ICS-3000 Model SP-1), Dionex CSRS Ultra 4mm self-regenerating suppressor, conductivity detector, and an Ion Pac CS12A analytical column. Inorganic anions as well those from carboxylic acids (formate, acetate, oxalate, carboxylic di- lactate, succinate, and glutarate) were analyzed using a Dionex ICS-5000+ IC, which was equipped with a gradient pump (ICS-3000 Model SP-1) and AMMS 300 MicromembraneTH suppressor and conductivity detector. The guard column and analytical column were Dionex IonPac™ AG11-HC and Dionex IonPac™ AS11-HC, respectively. The MDLs for carboxylates varied between 0.88 and 4.05 ng m^{-3}, were lowest for formate and highest for succinate at a nominal sampling volume of 24 m^3 for each typical 24 h PM sampling period.

Additionally, in summer samples sugars (glucose and mannose) and anhydrosugars (levoglucosan and mannosan) were determined using a Dionex ICS-5000+ IC equipped with a pulsed amperometric detector, a CarboPac MA1 guard column and an anion-exchange analytical column, and a Dionex ICS-5000 Electrochemical Detector. The MDLs for sugars and anhydrosugars varied between 1.59 and 3.35 ng m^{-3}, were lowest for levoglucosan and highest for glucose at a nominal sampling volume of 24 m^3 for each typical 24 h PM sampling period.

In precipitation samples the concentrations of SO_4^{2-}, Cl^-, NO_3^- and H^+, Ca^{2+}, Mg^{2+}, Na^+, K^+, NH_4^+ ions as well as hydrogen carbonate (HCO_3^-) and pH were measured. HCO_3^- and pH were analyzed immediately after sampling. Precipitation samples were tested for pH using a pH-meter SP-701 (Suntex, Taipei, Taiwan) calibrated by standard pH solutions before measurements. H^+ concentration was calculated from pH values. Hydrogen carbonate was determined by acidimetric titration with 0.005N HCl by an ionmeter (Econics, RF). The concentrations of other cations and anions were analyzed by using ion chromatography on a JetChrom instrument (Portlab, Moscow, Russia). Detection limits varied between 0.02 mg/L for NO_3^-, Mg^{2+}, NH_4^+, and K^+, and 0.03 mg L^{-1} for SO_4^{2+}, Na^+ and 0.05 mg L^{-1} for HCO_3^-, Cl^-, Ca^{2+}.

2.4. Statistical methods

In order to compare PM_{10} and ion data from different seasons and check for similarities between seasons and variables, Mann-Whitney test (Mann and Whitney, 1947) and Spearman correlation indexes (Spearman, 2010) were used. We decided to use such tests, instead of the classical Student's *t*-test and Pearson correlation, because these are non-parametric. They allow the robust comparison even in the absence of normally-distributed data, as typically observed for atmospheric variables (Ott, 1990). For Mann-Whitney test, compositional data were divided into three groups, based on the three analyzed seasons, and for each variable the comparisons between each couple of seasons were

computed. Results are expressed in terms of *p*-values, used in this case as a "similarity index": *p*-values higher than the chosen significance level (0.05) indicates that the two compared variables are not statistically different, while *p*-values lower than 0.05 indicate a statistically relevant difference.

Method based on the bivariate polar plot (Carslaw and Ropkins, 2012) shows how the concentration of species varies jointly with wind speed and wind direction in polar coordinates. This approach allows to trace the source location, preferably at scale ~1-10 km where the wind direction is remaining quasi-constant while the calculations of air mass transportation provides a limited support thanks to the low spatial resolution of the model employed (Carslaw and Beevers, 2013). The highest values of concentrations identify the directions of emission source.

Backward trajectories (BWT) were generated using NOAA HYbrid Single-Particle Lagrangian Integrated Trajectory (HYSPLIT) model of the Air Resources Laboratory (Stein et al., 2015), with coordinate resolution equal to 1° × 1° of latitude and longitude. The potential source areas were investigated using 3 days back for air masses arriving each one hour at 500 m height above sea level (A.S.L.). BWTs were calculated in 1 hour for all periods of sampling.

Cluster analysis of trajectory data is an effective method of grouping the origin-like trajectories by combining the geographically close data, it takes into account the features of seasonal atmospheric circulation. The angular method is selected in which the matrix of angular distances shows how similar are two points of the BWT in dependence on their angle with respect to the initial location (Cui et al., 2021). Fire information was obtained from Resource Management System (FIRMS), database MODIS (https://firms.modaps.eosdis.nasa.gov/map), operated by the NASA/GSFC Earth Science Data Information System (ESDIS).

The scavenging ratio is a parameterization of the loss rate for gas or aerosol particles from the atmosphere by their incorporation into larger drops. This factor can be calculated by taking into account the volumes or masses of the chemical species being exchanged (Engelmann, 1971; Kasper-Giebl et al., 1999). The scavenging ratio in our study is the quotient of the concentration of ions in precipitation related to the concentration of those ions in aerosols. The scavenging ratios for each ion (ω) were calculated using the following formula:

$$\omega = (C_p/\rho_p)/(C_a/\rho_a), \quad (1)$$

where C_p is the ion concentration in precipitation, μg L^{-1}, C_a is the concentration of the same ion in aerosols, μg m^{-3}, ρ_p is the density of the precipitation, 1.0 kg L^{-1}, ρ_a is the density of the air. Air density was assumed to be constant during all sampling periods (1.2 kg m^{-3}). With formula (1), it is possible to estimate the impact of rainfall for the different chemical species**.** In this work we have limited our calculation to season averages and to SIA ions, since their origin is more safely attributable to wet

deposition as the aerosol scavenging processes; the other ion species may come from dry deposition which cannot be solved using a bulk precipitation collector.

Source apportionment was performed for both particulates and precipitation by factor analysis using the Varimax algorithm (Van Espen and Adams, 1983), that is an extension of principal component analyses (PCA) with a rotation of the principal components space to convert the PCs into factors. In this way, each factor can be considered as the common source for the variables having higher loading values for that factor. This method was preferred to other more efficient models such as Positive Matrix Factorization owing to statistical constraints dictated by the limited number of observed parameters (Hopke, 2016).

3. Results and discussion

3.1. Aerosol data overview

3.1.1. PM_{10} and meteorological parameters overview

Table S1 presents the seasonal statistics of meteorological variables. Springtime of 2018 and summertime of 2019 with mean temperature 14 ± 4.7°C and 18.7 ± 3.8°C, respectively, corresponded to the warm period while autumn with low mean temperature 3.2 ± 5.4°C belong to the cold period. The season with the highest precipitation (6.53 ±1.3 mm) was summer. Time series of PM_{10} mass in three seasons, i.e., spring 2018, summer 2019, and autumn 2019 was shown in Figure 2. PM_{10} did not exceed the EU threshold of 50 μg m^{-3} during any day if not in rare cases. The plot of PM_{10} vs. the main meteorological variables reveals that higher values were detected in association with periods of low or no precipitation (Figure 2a), and low wind predominant from the southwest (Figure 2b). The wind rose for the studied period is shown in Figure 2c, confirming westerly and south-westerly winds with speeds between 0.5 and 2.5 m s^{-1}, similar to the predominant wind direction for the MO MSU reported by (Chubarova et al., 2014). No particular correlation was observed between PM_{10} and temperature (Figure S1a). Lower PM_{10} was encountered in connection with lower pressure (Figure S1b), usually coinciding with higher precipitation (Figure 2a) and relative humidity (Figure S1c), responsible for aerosol wet scavenging, in agreement with the PM_{10} wet removal. The biggest differences between meteorological parameters were found for temperature and relative humidity by boxplots in Figure 3.

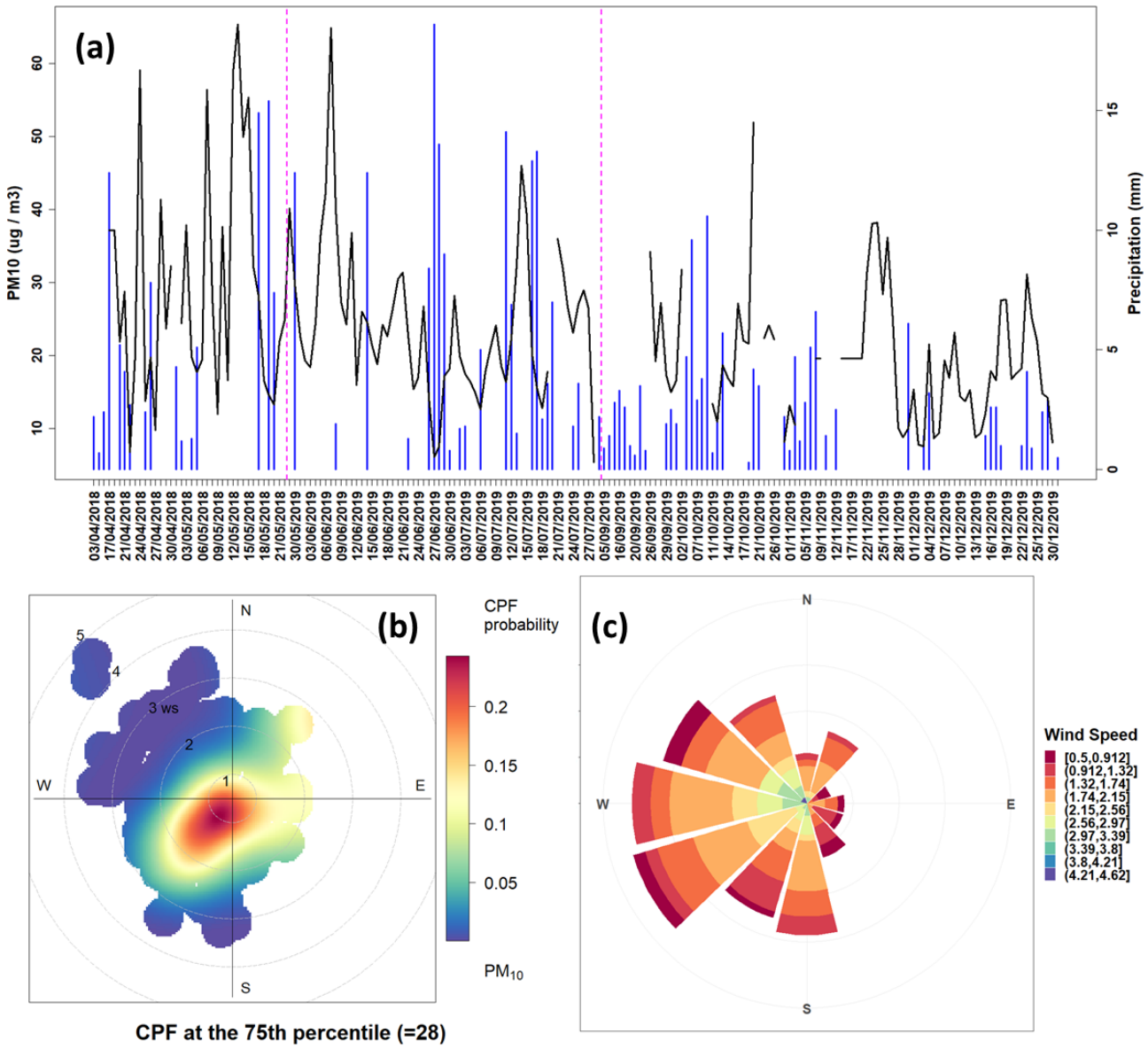

Figure 2. a) Time series of PM_{10} (black lines) and precipitation (blue bars), dashed lines indicate the separation between three seasons; b) CPF bivariate polar plots showing the wind speed (ws) and wind direction dependence of PM_{10} concentration at 75^{th} percentile, radial axis for wind speed in m s^{-1}; c) wind rose for the whole period of study.

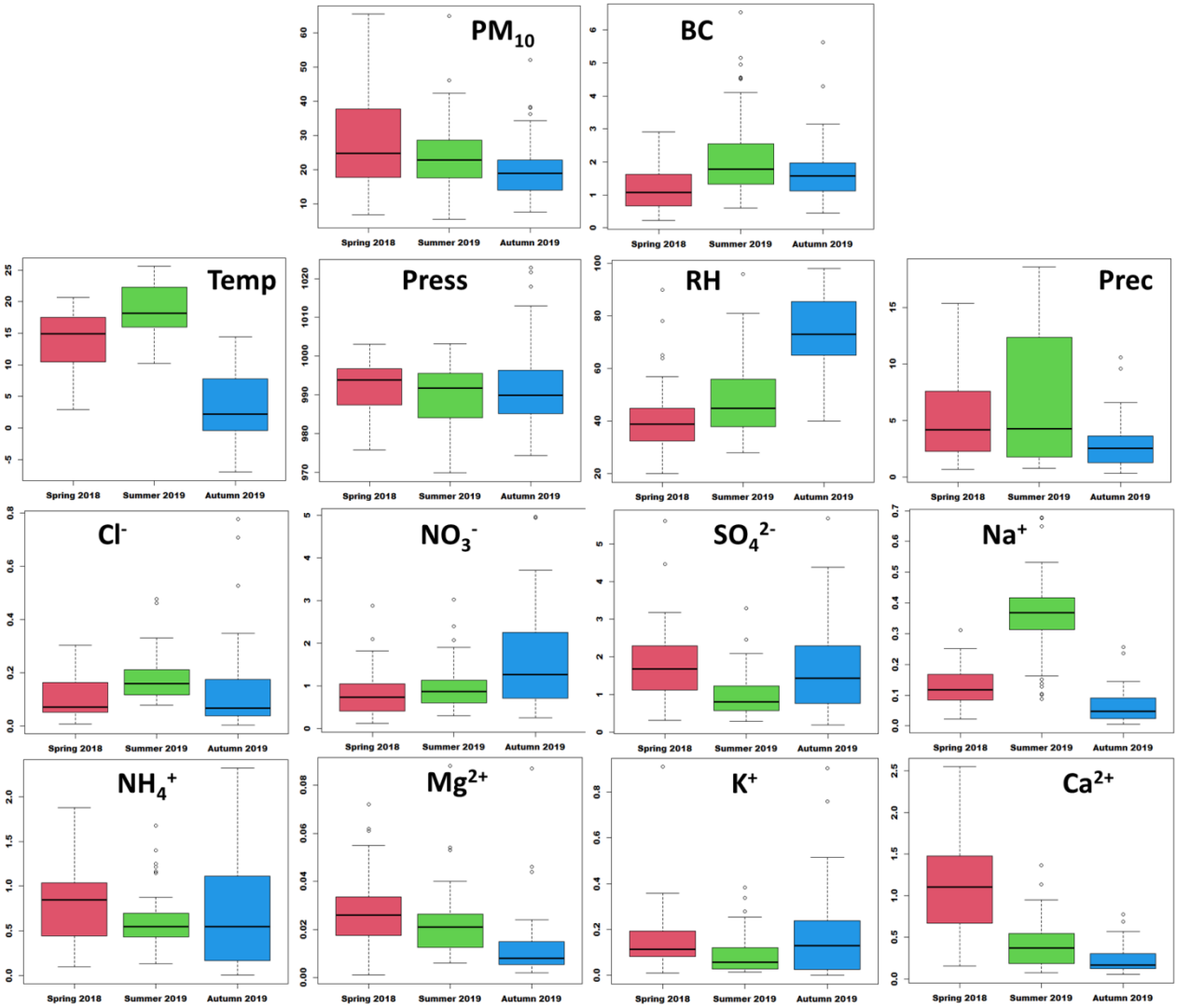

Figure 3. Boxplots of aerosol PM_{10}, BC, temperature (Temp, °C), pressure (Press, hPa), relative humidity (RH, %), and Precipitation (Prec, mm), and inorganic ions concentrations (μg m^{-3}) for spring 2018, summer 2019, and autumn 2019. Units of measure are the same of Table S1. Red, green, and blue boxes indicate spring, summer, and autumn, respectively.

3.1.2. Descriptive statistics

Basic statistics on seasonal concentrations of PM_{10}, inorganic ions (SO_4^{2-}, NO_3^-, Cl^-, Ca^{2+}, K^+, Na^+, and Mg^{2+}), carboxylic acids, and sugars is shown in Table S1 for the whole period of study. Oxalate and nitrite (NO_2^-) could be measured above DL additionally to inorganic ions in spring, and in autumn and summer, respectively. Carboxylates (oxalate, acetate, formats, lactates, glutarates and succinates) as well as sugars (mannose, glucose) and anhydrosugars (levoglucosan and mannosan) were considered for summertime only. Also, total inorganic ions (TII), total organic ions (TOI) and total sugars (TS) are estimated in Table S1.

Maximum mean PM_{10} (33.5±28.2 μg m^{-3}) was found in spring and minimum (19.5±8.6 μg m^{-3}) in autumn. Statistically significant difference was estimated between autumn as compared to other two seasons. In both spring and autumn mean concentrations for inorganic anions and cations was found as following: SO_4^{2-}>NO_3^->Cl^- and Ca^{2+}>K^+>Na^+>Mg^{2+}. In summer this tendency is the same, except for Na^+, higher than K^+.

Boxplots for inorganic ions are shown in Figure 3. Na^+ showed the largest variability between seasons, with a median of 0.37 μg m^{-3} and maximum of 0.67 μg m^{-3} in summer and a median of 0.05 μg m^{-3} and minimum of 0.01 μg m^{-3} in autumn, respectively. Its variability is well-captured by Mann-Whitney tests comparing chemical values between seasons: *p*-values are all statistically significant (< 10^{-4}), indicating significant differences between all couple of seasons. A similar behavior was found also for Ca^{2+}, although in this case a maximum (1.11 μg m^{-3}) in spring and a minimum (0.16 μg m^{-3}) in autumn were observed, all Mann-Whitney *p*-values are statistically significant. K^+ is different by the highest median of 0.11 μg m^{-3} and maximum in spring of 0.99 μg m^{-3}, and in autumn (0.124 and 0.76 μg m^{-3}) with significant differences (*p*-value < 0.5) in summer. Median Cl^- (0.17 μg m^{-3}) and SO_4^{2-} (1.0 μg m^{-3}) also demonstrate the significant differences in summer while similarities are found for these ions in the other seasons. Median NO_3^- (1.6 μg m^{-3}) and Mg^{2+} (0.12 μg m^{-3}), instead, showed significant differences in autumn as compared to other seasons, while a median NH_4^+ (0.8 μg m^{-3}) exhibited a slightly significant difference (*p*-value = 0.04) only when comparing spring and summer values.

Massive contribution of measured species to PM_{10} for each season is shown in Figure 4. Total inorganic ions (TII) constitute the largest fraction of aerosol mass in the cold period reaching a maximum of 27% in autumn, and a minimum of 16.5% in summer. Sulfates and nitrates dominate among the major anion components, with maximum contribution of 38 and 34% to TII in autumn. Cations are mainly represented by calcium and ammonium. Ca^{2+} had a maximum of 21% in spring and minimum of 5% in autumn. Seasonality of NH_4^+ was not prominent, ~15-17% in any season. A lower though significant fraction of inorganic ions in TII was represented by sodium and chloride; in summer the percentage of both Cl^- and Na^+ approached their maxima respectively of 5 and 11%, dropping to minima of 1.6 and 2% in autumn, respectively. Finally, maximum of K^+ fraction of 3% was observed in spring and autumn.

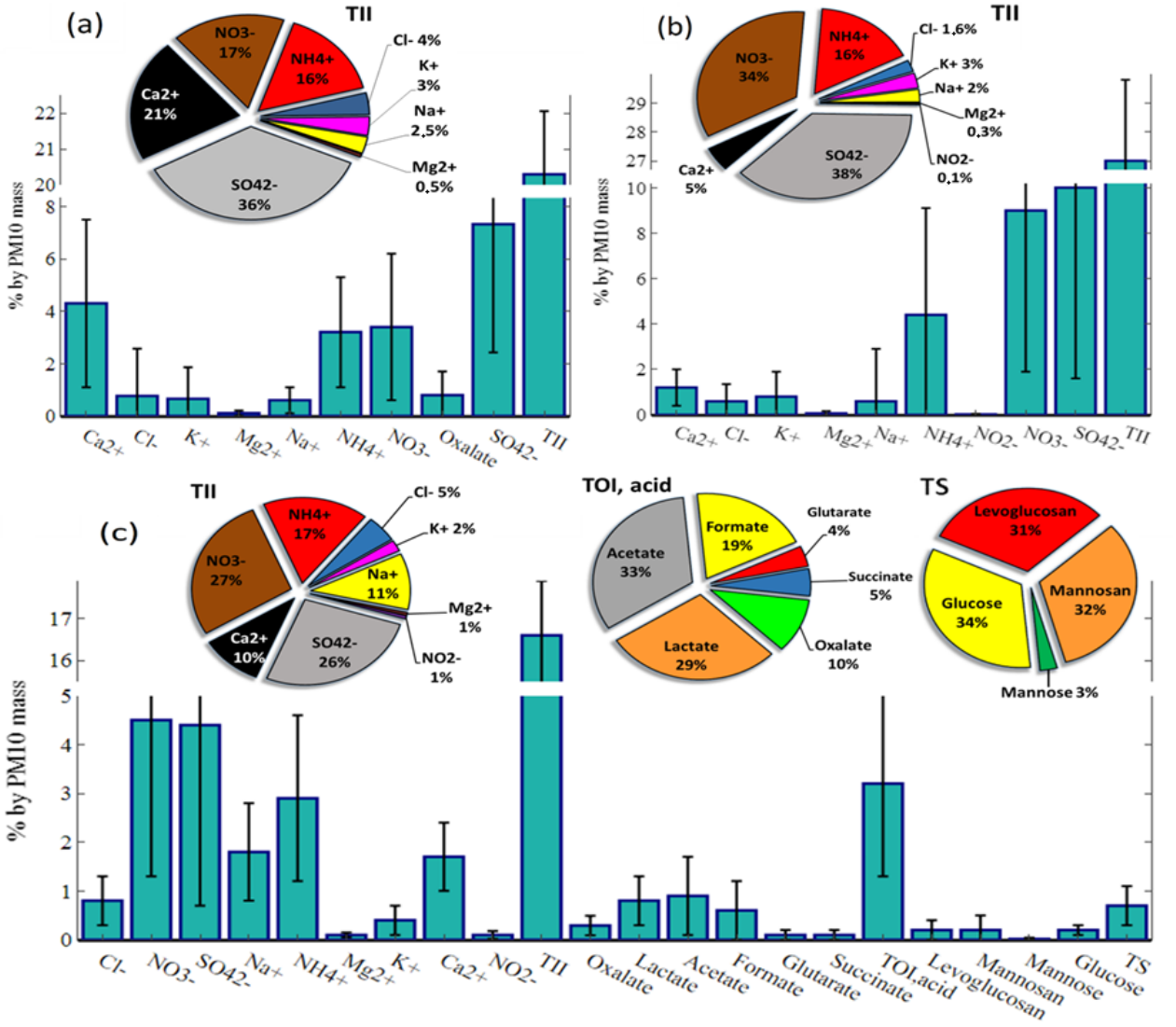

Figure 4. Percentage contribution in PM10 mass of inorganic ions and oxalate in spring 2018 (a), of inorganic ions and NO2- in autumn 2019 (b), and of inorganic ions, organic ions, sugars and anhydrosugars in summer 2019 (c). Contribution of total inorganic ions (TII), total organic ions (TOI) and acids, and total sugars (TS) including anhydrosugars is shown. Pie diagrams show the relative abundance of individual measured species in total.

In European urban areas, ammonium sulfate and nitrate concentrations may reach up to 21-28% of PM_{10}, owing to the extensive use of combustion at all the scales from industry down to domestic and individual uses (Putaud et al., 2010; Tositti et al., 2014). In Moscow urban background we have obtained the maximum contribution of ammonium sulfate and nitrate to PM_{10} around 15% in the cold period.

Summer species analyses showed that total inorganic fraction in PM_{10} was higher (16.5%) than total carboxylates (3.5%), and total sugars and anhydrosugars (0.8%). Acetate and lactate dominated total organic ions (TOI), 33% and 29%, respectively. Acetate constitutes 1% to PM_{10} mass in summer

399 samples. Levoglucosan and mannosan were the most prominent components of total sugars with
400 respectively 31% and 32%.
401
402 **3.1.3. Comparing Moscow PM data with other large cities**
403 Aerosol sources are seasonally modulated by a number of meteorological factors, e.g., precipitation,
404 atmospheric circulation as well as solar radiation, all influencing the planetary boundary layer height
405 and, therefore, air pollutant concentrations. Urban emissions may be also influenced by seasonal
406 variability, as in the case of domestic heating. In Table 1, data obtained for Moscow urban background
407 are compared with a few large cities such as Amsterdam, London, Athens, and Paris. The comparison
408 was carried out with urban background sites of big cities taking place also at the similar northern
409 latitudes as Moscow. Mean PM_{10} in Amsterdam (Hama et al., 2018) is slightly lower than Moscow
410 but SIA concentrations are higher. SIA concentrations in London are also higher (Beccaceci et al.,
411 2015). In Athens NO_3^- concentrations are comparable with Moscow while other SIA are higher. The
412 average PM_{10} in Paris suburbs is almost twice higher while the concentrations of SIA are 3-12 times
413 higher (Srivastava et al., 2018). Continental Toronto downtown, that is found at a similar latitude
414 than Moscow but is influenced by the Great Lakes, shows SIA (Jeong et al., 2020) comparable to
415 those observed in Moscow. Here we note that data for Toronto and Athens are presented for $PM_{2.5}$.
416 However, the comparison hold for SIA species may be reasonably considered because the SIA
417 populating the submicron range is common to both PM_{10} and $PM_{2.5}$.
418 Despite Moscow has the largest population among European and Canadian cities of our comparison
419 (with exception of London closer with its 9 million of inhabitants) though their size is not comparable,
420 our data shows that Moscow urban background has the lowest SIA content with minima of SO_4^{2-} and
421 NH_4^+, and comparable NO_3^-. Such finding is well related to a fact that nitrogen oxides constitute a
422 large fraction of gaseous atmospheric pollution in Moscow , and their concentration is comparable to
423 most of largest cities in industrialized countries while the average concentration of sulfur dioxide,
424 ozone, and carbon monoxide is much lower than in the majority of world megacities (Elansky et al.,
425 2007). The reason for that is the dominant using of gas as a fuel, leading mainly to the emissions NO_x
426 and CO from heat and power plants (Elansky, 2014).
427 Na^+ and Cl^- concentrations in all the cities mentioned above with marine climate are higher than in
428 Moscow a few times, indicating direct sea salt impact on their airsheds. Under ordinary circulation
429 conditions, sea salt cannot exceed a few kilometers from the coast-line inward. In Toronto (Srivastava
430 et al., 2018), Na^+ and Cl^- are significantly less, revealing the absence either sea-salt or road
431 management impact on the ion composition. The similar trend of strongly higher Mg^{2+} concentrations
432 are found for coastal cities, probably the indication of the impact of sea salt aerosols on water-soluble

species as well. Road salt aerosol driving wintertime atmospheric chlorine chemistry have been observed for inland cities (McNamara et al., 2020) and related to pseudo-marine factor relating to winter street management (Tositti et al., 2014). Thus, Cl^- and Na^+ concentrations at the MO MSU site can be attributed to the impact of de-icing agents (DIAs) on aerosol composition in agreement with previous work by Eremina et al. (Eremina et al., 2015). Indeed, icy winters with long-lasting snow deposits require an intensive road management in Moscow to prevent traffic inconveniences. The composition of solid and liquid DIA used in Moscow megacity is dominated by NaCl salts, as reported in Supplementary Material. DIAs resuspension by traffic-induced turbulence significantly alter the snow composition along the roadsides (Vlasov et al., 2020). Near the MO MSU, soil salinization persists throughout the year and practically does not depend on the moisture regime affecting aerosol composition by soil resuspension in a continuous way and a modulation controlled by local circulation.

Mean PM_{10} in Moscow is comparable with continental large cities such as Berlin (Wieprecht et al., 2004) and Prague (Schwarz et al., 2019), and slightly lower than in Sofia (Hristova et al., 2020) and Bucharest (Perrone et al., 2018). All mentioned cities are characterized by higher SO_4^{2-} and NH_4^+ concentrations than in Moscow. NO_3^- is higher for Prague and Berlin, and comparable for Sofia and Bucharest. Transport of marine aerosols and impact of road salt along with aged sea salt increases Na^+ and Cl^- concentrations in Sofia (Hristova et al., 2020). In Prague, road salt along with aged sea salt provide the similar concentrations as in Moscow (Schwarz et al., 2019). Moreover, in Prague, the concentrations of Mg^{2+} is comparable while Ca^{2+} is two times lower than in Moscow. In Budapest, Na^+ concentrations are lower, and Mg^{2+} concentrations are comparable to Moscow. K^+ is only one ion which concentration data for Moscow and other cities are very similar, an exception is Sofia where three times higher pollution by potassium related to residential heating is observed.

Although a longer sampling campaign would be required to draw conclusive considerations, our data indicate that the pollution in Moscow is comparable, if not lower, than that of also smaller cities. Paris and London, moreover, have significative higher pollution, but with certainly lower dimensions and populations.

Table 1. Mean PM_{10} and ions concentrations, in μg m^{-3}, in Moscow and large European and North America cities over periods indicted. Sites of comparison are described.

City, period	PM_{10}	Cl^-	NO_3^-	SO_4^{2-}	Na^+	NH_4^+	Mg^{2+}	K^+	Ca^{2+}	site
Moscow, Russia Apr – May 2018, Jun – Dec 2019	23.3	0.14	1.20	1.46	0.18	0.69	0.02	0.13	0.48	urban background
Amsterdam, Netherlands Apr 2013 – May 2014	20.7	0.98	4.79	2.2	0.86	1.75	0.13	0.10	0.27	urban background

London, UK Jan 2013 – Dec 2013	--	1.34	3.41	2.16	1.05	1.25	0.14	0.09	0.39	urban background
Paris, France 6-21 March 2015	49.0	0.58	14.4	4.3	0.41	5.66	0.06	0.14	0.86	suburban background
Athens,Greece June 2005-Sep 2006	24.2*	0.26*	1.42*	4.19*	0.73*	1.32*	0.12*	0.18*	1.2*	suburban background
Toronto, Canada Mar 2004 – May 2014	13.0*	0.03*	1.70*	1.88*	0.04*	0.91*	0.01*	--	--	Downtown
Sofia, Bulgaria Jan 2019 – Jan 2020	30.9	0.31	1.87	3.03	0.37	0.75	0.12	0.36	0.76	urban background
Budapest, Hungary Feb 2015 – May 2015	29.9	--	1.9*	2.0*	0.13*	1.2*	0.02*	--	--	urban background
Prague-Libuš, Czech Rep. Apr 2008 – Mar 2009	26.7	0.22	3.15	2.86	0.16	1.67	0.03	0.13	0.22	suburban background
Berlin, Germany Sep 2001 – Sep 2002	22.3	--	2.4	3.9	--	1.8	--	--	--	urban background

Note. *Data are given for $PM_{2.5}$

3.2. Aerosol data analysis

3.2.1. Cations and anions balance

For sake of electroneutrality constraints, cations and anions have been analyzed for their charge balance. Ion data, converted into equivalents, show a deficit of anions in spring and summer, 33% and 35%, respectively (Fig. S2). This fact may be ascribed to carbonate ions, that were not analyzed directly. Their concentration was calculated from calcium and magnesium concentrations (Alastuey et al., 2004; Popovicheva et al., 2020d; Tositti et al., 2014) attributed to the mineral components associated to soil resuspension (Chow et al., 2015). Once added CO_3^{2-} to anions, linear regressions are computed for three seasons (Fig. 5). Table 2 shows R^2, slopes, and intercepts, and their relative standard deviations, σ, for the three seasons. Results indicate that spring aerosol is substantially electroneutral with the slope and intercept not significantly different from their ideal values of 1 and 0, respectively. Summer data, instead, show a slope slightly, but significantly different from 1 (*p*-value = 0.01). This indicates a slight excess of cations, but such a low difference, given that the intercept is not significantly different from 0, is most likely due to the experimental uncertainties, characterizing summer aerosol as almost neutralized. Autumn regression, instead, shows both slope and intercept significantly different from 1 and 0 (*p*-values 0.005 and 0.0001). This suggests an excess of anions, probably due to the presence of not neutralized H^+ which can be a result of the gas to particle conversion of SO_2 and NO_x to their respective acids and ammonium salts (not measured and therefore unaccounted in the charge balance), due to a temporary reduction of alkaline substances such as gaseous NH_3. It is to note that for Moscow atmosphere this component may include not only actual soil and road components, but also the additional carbonate fraction and, what's more, $CaCl_2$

in DIA used for road management leading to a not predictable split of Ca and consequent bias in the charge balance (Eremina et al., 2015; Vlasov et al., 2021).

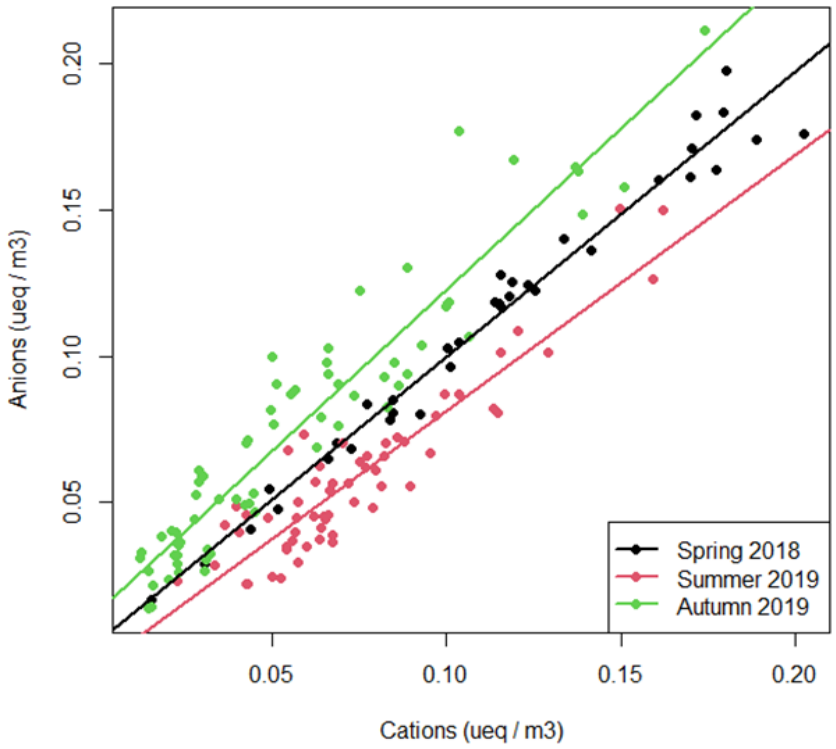

Figure 5. Linear regressions of anions vs cations for spring 2018, summer 2019, and autumn 2019 with the contribution of CO_3^{2-} added to anions.

Table 2. Regression lines parameters for ion charge balance for three seasons.

Season	R^2	Slope	σ_{slope}	Intercept	$\sigma_{intercept}$
Spring 2018	0.97	0.97	0.03	0.002	0.0035
Summer 2019	0.84	0.87	0.05	-0.006	0.0039
Autumn 2019	0.89	1.10	0.04	0.012	0.0032

3.2.2. Chloride depletion

We check for the occurrence of chloride depletion in Moscow urban background, deriving from the likely interactions of HNO_3 with NaCl (Hoffman et al., 2004; McNamara et al., 2020). The reaction involved is the following:

$$NaCl + HNO_{3(vap)} \rightarrow NaNO_3 + HCl_{(gas)} \quad (2)$$

It was previously shown that the appearance of hydrogen chloride in the atmosphere of Moscow is the result of heterogeneous multiphase chemical reactions, including the above one, with the participation of DIAs (Eremina et al., 2015) .

In order to evaluate the chloride depletion in three seasons, regressions were computed using Na^+ as independent variable, owing to its remarkable chemical stability in the environment, and Cl^- as the

dependent variable. The results are reported in Figure 6 and Table 3. Ion concentrations reveal a poor but positive ($R^2 > 0.4$) correlation in spring and autumn with slopes of 0.87 and 2.02, respectively. Both slopes are far from 1.54, the value expected for NaCl composition. In spring, Cl^- concentration is less than expected in sodium chloride, demonstrating a feature of chlorine depletion following the snow melt and the remobilization of DIA in road dust.

In summer, the correlation between Cl^- and Na^+ is negative, suggesting a significant influence of reaction (2) in displacing chloride from sodium chloride. Probably, DIAs are not washed off efficiently by snow thawing and runoff as soon as the weather becomes milder, allowing for its aerosolization at the inception of warmer and drier conditions in summer. NaCl resuspension is promoted by both a significant low-level turbulence and dryness and the required photochemistry leading to HNO_3 accumulation, less easily neutralized by ammonia which reacts preferably to H_2SO_4 (Hewitt, 2001; Seinfeld and Pandis, 2016).

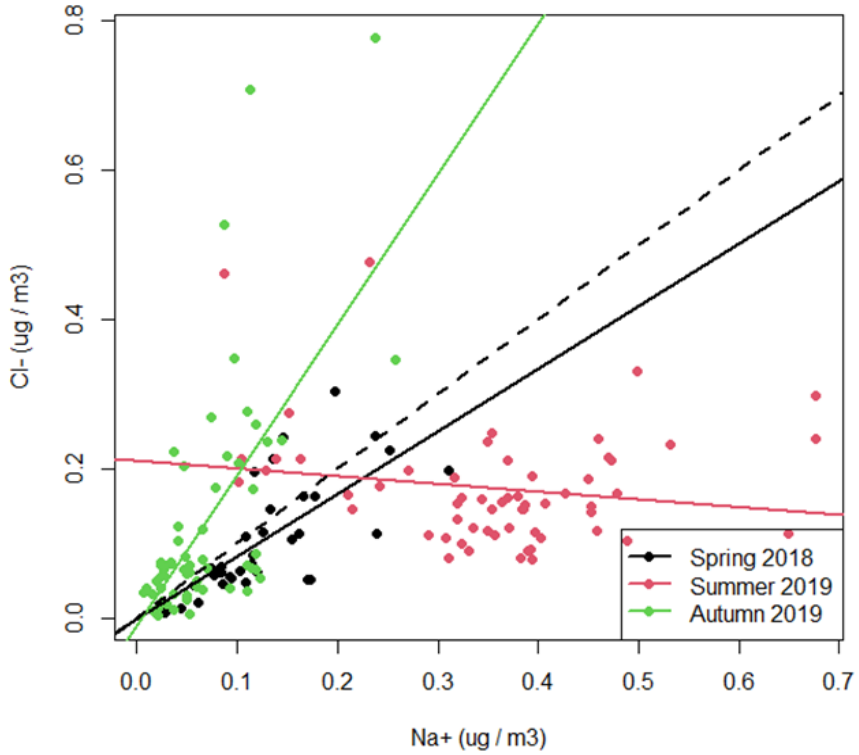

Figure 6. Correlation of Na^+ and Cl^- for the three seasons. Dashed line corresponds to concentration ratio of Na^+ and Cl^- = 1:1.

Table 3. Regression lines parameters for chloride depletion in three seasons.

Season	R^2	Slope	σ_{slope}	Intercept	$\sigma_{intercept}$
Spring 2018	0.49	0.87	0.14	-0.003	0.02
Summer 2019	0.01	-0.10	0.08	0.21	0.03
Autumn 2019	0.41	2.02	0.31	-0.01	0.025

3.2.3. Secondary inorganic aerosol (SIA)

SIA derives from the oxidation of SO_2 to H_2SO_4 and of NO_x to HNO_3, respectively, under the influence of photochemically driven oxidation processes (Hewitt, 2001). These reactions are followed by variable degrees of neutralization by two alkaline substances, i.e. gaseous NH_3, the most abundant atmospheric alkaline substance, and to a lesser extent $CaCO_3$ of mineral origin (Fountoukis and Nenes, 2007; Heal et al., 2012; Karydis et al., 2020; Tositti, 2018). It is to note that the neutralization of H_2SO_4 by NH_3 is thermodynamically favored as compared to the analogous reaction with HNO_3, while NH_4NO_3 is less thermally stable, both conditions promoting the availability of HNO_3 for reaction (2) and the subsequent chloride depletion.

Lai et al. (Lai et al., 2007) proposed two methods to evaluate the degree of neutralization of ammonia as sulfate or nitrate by using the correlation between the concentration of NH_4^+ and that calculated from the concentrations of SO_4^{2-} and NO_3^-. Both methods are based on stoichiometric considerations and are based respectively on the neutralization of H_2SO_4 and HNO_3 by ammonia as NH_4NO_3 and NH_4HSO_4 (method 1), or as NH_4NO_3 and $(NH_4)_2SO_4$ (method 2). In our work, we used nss-SO_4^{2-} fraction instead of total SO_4^{2-}. The results obtained are depicted in Figure 7, Table 4 shows the regression results. According to Lai et al., the good correlations ($R^2 > 0.7$) and intercepts not significantly different from zero indicate that sulfates and nitrates are fully neutralized by ammonia in spring and summer. In autumn, the intercept is significantly higher than 0, sulfate and nitrate are not fully neutralized by ammonia, but other cations (as Mg^{2+} and Ca^{2+}) contribute to the equilibrium. Ammonia, indeed, is supposedly less abundant in autumn owing to a decrease in biogenic activities and to soil capping due to snow cover as soon as the cold season proceeds. These seasonal features of ammonium participation in the formation of SIA and their further washing out by precipitation lead to the fact that the share of ammonium in the total amount of ions in the snow cover is on average about 6% (Eremina and Vasil'chuk, 2019), while in precipitation during the warm period it averages 11-12% (Eremina, 2019). The slope closer to 1, found by method 2, suggests that nitrate and sulfate exist mostly as NH_4NO_3 and $(NH_4)_2SO_4$ in all seasons.

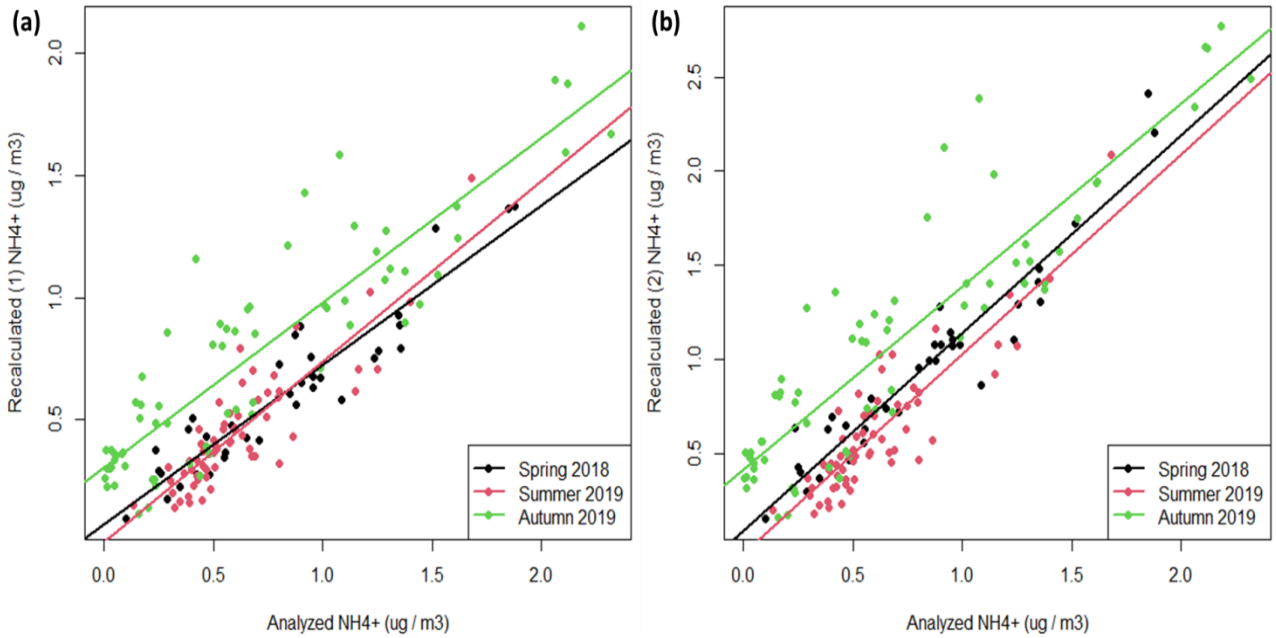

Figure 7. Regression lines of recalculated vs analyzed NH_4^+ concentrations according to a) method 1 and b) method 2 (Lai et al., 2007).

Table 4. Parameters of the regression lines for neutralization of sulfates, nitrates, and ammonia as NH_4NO_3 and NH_4HSO_4 (method 1), and as NH_4NO_3 and $(NH_4)_2SO_4$ (method 2).

Method 1	**R^2**	**Slope**	**σ_{slope}**	**Intercept**	**$\sigma_{intercept}$**
Spring 2018	0.87	0.65	0.043	0.072	0.040
Summer 2019	0.74	0.74	0.056	-0.002	0.038
Autumn 2019	0.79	0.67	0.042	0.305	0.039
Method 2					
Spring 2018	0.90	1.05	0.057	0.087	0.053
Summer 2019	0.76	1.06	0.076	-0.036	0.052
Autumn 2019	0.80	0.97	0.058	0.413	0.054

3.3. Potential source analyses

3.3.1. Anemological analysis

Meteorological factors contribute significantly to variability of the ionic content in aerosols (Dadashazar et al., 2019). Relationships among the source factor and wind direction and speed, i.e. anemological analysis, are derived from polar plots (Saraga et al., 2021). Figure 8 shows the bivariate concentration polar plots during spring 2018, summer and autumn 2019, providing a graphical representation of the source origin for the MO MSU site. Map of Figure 1 depicts the MO MSU sampling site located in the southwest sector of Moscow, where industrial facilities are placed within a distance up to 10 km, including thermal power stations, thermal stations, mechanical engineering, metallurgical, food, reinforced concrete, chemical and pharmaceutical factories.

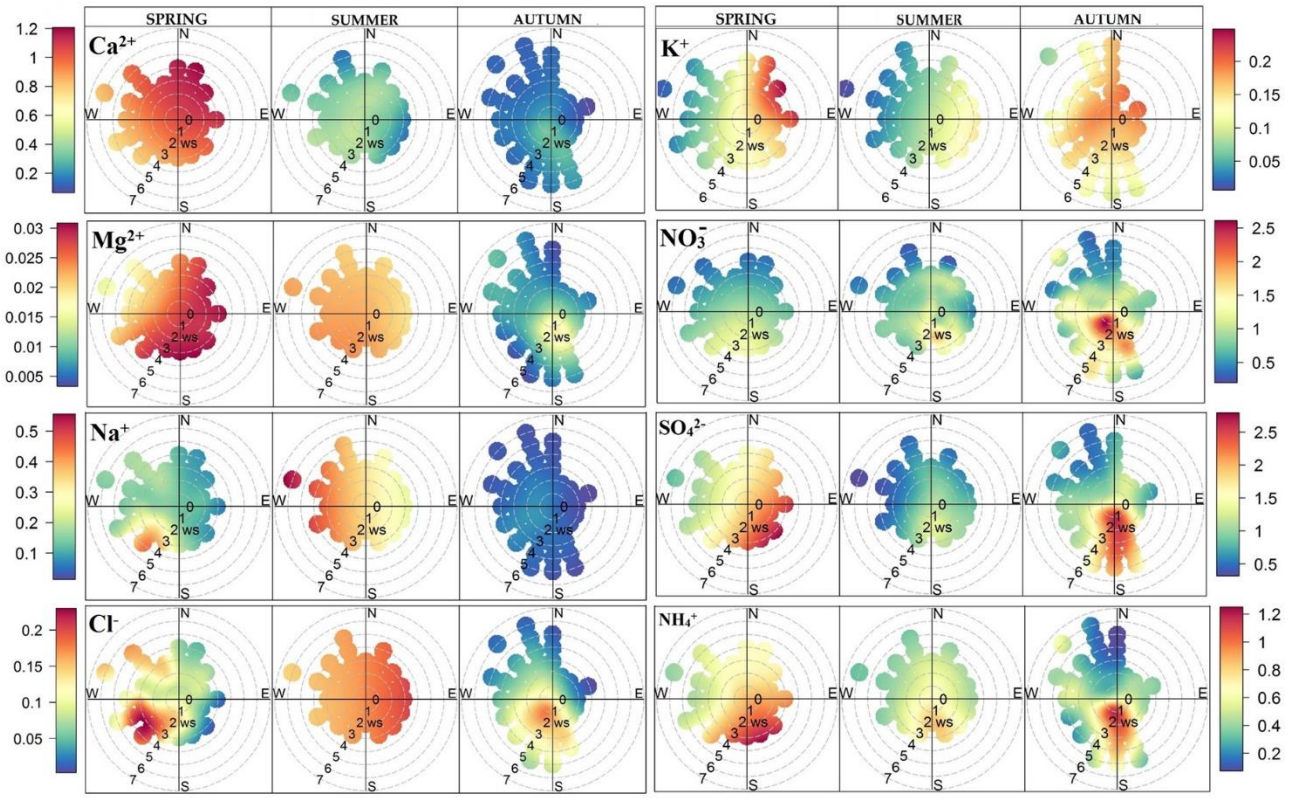

Figure 8. Concentration bivariate polar plots showing the wind speed and wind direction dependence during spring 2018, summer and autumn 2019. The radial axis is wind speed in m s^{-1} and the color scale is the concentrations in μg m^{-3}.

Polar plots of SO_4^{2-} and NH_4^+ show a very similar pattern indicating the same origin for ammonium sulfates and reflects the high correlation between these ions as a result of the significant thermodynamic stability of ammonium sulfates originated from SO_2 gas-to-particle conversion (Hewitt, 2001). In spring and autumn, they indicate the pollution sources in the southeast where the most industrially developed area takes place in Moscow (Bityukova and Saulskaya, 2017). Prevailing winds were from north and northwest in summer, therefore the MO MSU site is not downwind the heavily impacting sources as in spring and autumn.

High concentrations of NO_3^- (about 1.5 μg m^{-3}) in spring and summer are observed at weak wind conditions when non-buoyant ground-level sources such traffic are important. Increasing wind speed generally results in lower concentrations due to dispersion and mechanical turbulence. In autumn, NO_3^- increases probably due to the centralized heating system operation when the MO MSU site is downwind from southwest stacks of the large industrial zone (in particular, from the thermal power stations (Fig. 1)) as well as from the southeast industrial region.

Cl^- and Na^+ polar plots in spring indicate high concentrations, above 0.2 and 0.32 μg m^{-3}, respectively, from southwest at wind speeds higher than 2 m s^{-1}. In fact, it coincides with heavily trafficked roads

southwest MO NSU where efficient road management aiming at reducing snow/ice deposits in the cold period is carried out systematically. In summer, the amount of salts in soil interstitial water drops by 2-7 times (Nikiforova et al., 2014). Also, Cl^-, Na^+ and NO_3^- decrease due to salt leaching, runoff, and absorption of nitrates by biota, but Ca^{2+}, Mg^{2+} and HCO_3^- increase because dust and crushed marble chips accumulation in the upper horizon (Kosheleva et al., 2018). Complete leaching of salts from the soil profile does not occur during summer, that leads together with soil solonetization to a progressive salinization of Moscow surface soils and to its substantial and everlasting availability to air-resuspension in the periods without snow cover (Nikiforova et al., 2017). Moreover, due to the greater amount of precipitation in summer compared to other seasons, Cl^- can migrates to the middle part of the soil profile while Na^+ fixed in surface soil horizon can be resuspended into the atmosphere. Na^+ polar plot in summer shows the resuspension of Na^+-enriched soil particles at any wind directions and speeds. Later, in autumn road salt is likely trapped in snow and ice with consequent scarce resuspension and no pronounced features of sources by polar plot.

For Ca^{2+} and Mg^{2+}, the high concentrations above 0.025 and 0.63 μg m^{-3}, respectively, in spring occurs from all the wind directions, relating to local source of soil resuspension after snow thaw. Ca^{2+} polar plot in summer shows additional source areas southwest and southeast, associated with intensive building activities in the New Moscow area. In the other seasons these ion sources are not clearly emerging.

K^+ can be originated from soil (mineral potassium) and biomass burning. It is to note that mineral potassium is less soluble than the corresponding fraction from biomass burning, owing to strong crystal lattice bonds in the rocks and minerals. K^+ in our experimental data, obtained from ion chromatography, represents most likely soluble potassium source. Thus, K^+ polar plot indicates biomass burning in spring from the east and in summer from the southeast at wind speeds higher than 2 m s^{-1}, with a likely dominating influence of remote sources in Moskovskaya Oblast as well as seasonal wildfires. Autumn plot, instead, indicates the presence of a major source of K^+ from all the directions and low wind speeds, though more intense from west and southeast. Since in autumn no wildfires are observed in the northern European part of Russia, the likely origin for K^+ is biomass burning in the region surrounding Moscow. The spectral dependence of the aerosol light attenuation observed in Popovicheva et al. (Popovicheva et al., 2022) supported the assessment for a contribution of biomass burning in the region around Moscow. We note that autumn is a cold season requiring domestic heating since September, it is recognized that the residential sector near Moscow employs wood for heating.

3.3.2. Backward trajectory analysis

Air pollutant transport relates to the atmospheric circulation and spatial distribution of regional sources. In spring and summer agriculture fires and wildfires may occur in the region around Moscow, thus providing the strong impact on city air quality. Additionally, the residential sector in Moscovskaya Oblact can impact with using of biomass for house heating and cleaning the gardens. Major directions of air mass transportations by BWT cluster analysis are shown in Figure 9. In spring, the main cluster C1 includes 36% of analyzed BWTs and indicates the northwestern and western direction as dominant. Clusters C2 (29%) and C3 (18%) of northwestern and southern directions support the prevalent air mass transportation, respectively. 17% of BWTs compose the cluster C4 from the north. In summer, the largest number of BWTs came from the northwestern direction (48%), they compose the cluster C1. The northern and southern directions include the cluster C2 and C3, characterized by 22% and 17%, respectively, while the trajectories coming from the southwest directions make a less significant percentage contribution to the cluster C4 (13%).

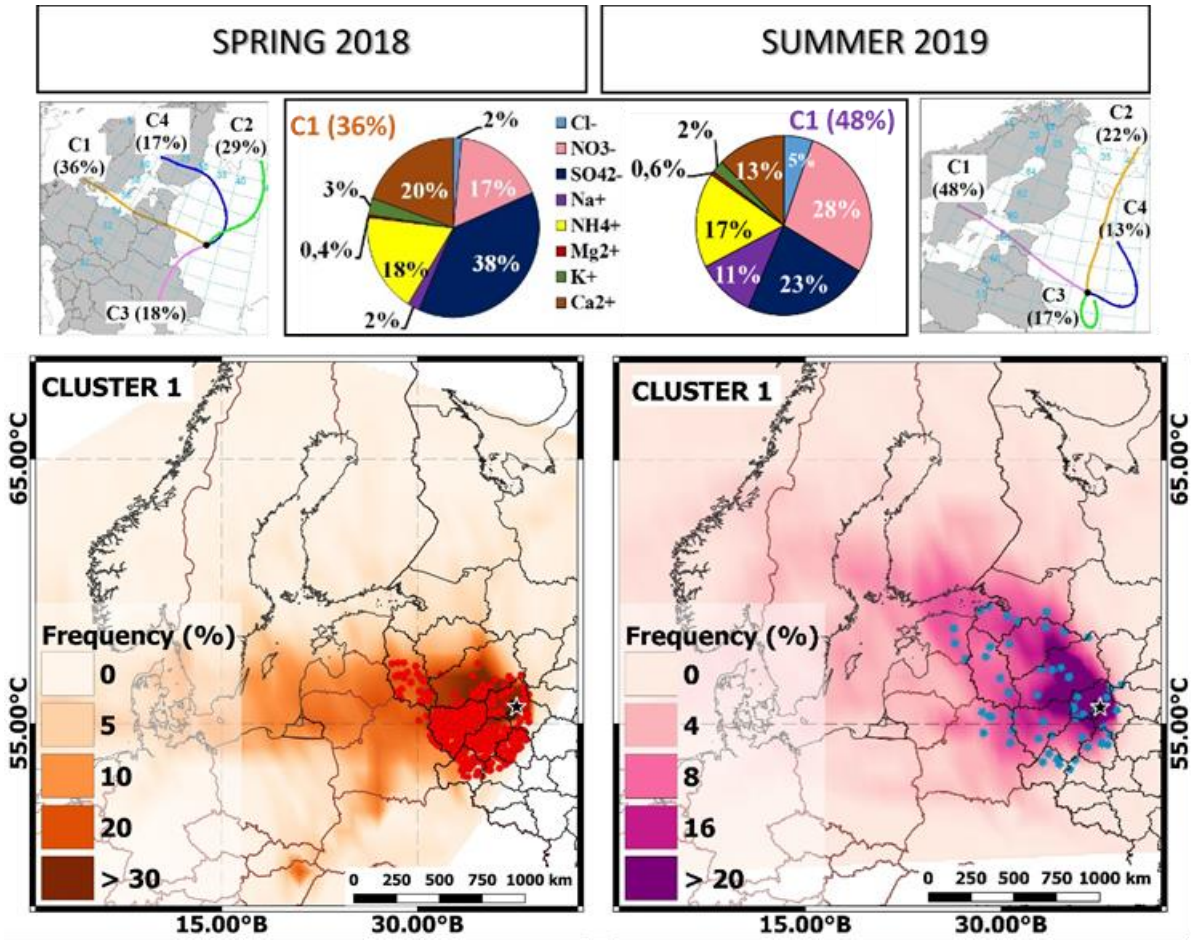

Figure 9. BTW cluster analysis and pie diagrams for ion concentrations which correspond to the trajectories within clusters C1 for spring 2018 (left) and summer 2019 (right) (top panel). 72-hour BWT frequencies of C1 cluster for spring 2018 (left) and summer 2019 (right) (bottom panel). Fire locations related to the time of BWT pass are indicated by stars, MO MSU site is marked by black star.

Pie diagrams in Figure 9 show ions concentrations related to trajectories within the clusters C1 of the prevalent air mass transportation for each season. SO_4^{2-}, NO_3^-, and NH_4^+ of 38%, 17%, and 18% and 23%, 28%, and 17% of total ion concentrations, compose the highest SIA source in the northwestern direction in spring and summer, respectively. Highest frequencies of BWTs in this direction relate to the area of large fires occurred in the European part of Russia and around Moscow in both seasons. High K^+ concentrations observed in this direction act as a marker of BB source impacted the air pollution of a megacity.

3.3.3. Varimax analysis: ions and BC sources

In order to obtain the aerosol source profile, the receptor modelling and factor analysis was applied (Hopke, 2016). In our study, Varimax analysis was computed using ion and BC data for the whole dataset, with the aim of finding the potential common sources. Five factors were chosen as the best solution, being the one explaining more than 80% of the total variance. Table 5 shows the Varimax loadings obtained by the model.

Table 5. Varimax loadings for ion and BC concentrations during the whole study period. Bold values correspond to the most representative variables for each factor. EV stands for the explained variance, F for a factor.

	F1	**F2**	**F3**	**F4**	**F5**
EV(%)	27.6	20.8	13.3	13.1	12.1
Cl^-	-0.050	0.040	0.089	**-0.898**	-0.123
NO_3^-	**-0.541**	0.187	-0.149	-0.236	0.048
SO_4^{2-}	**-0.550**	-0.102	0.044	0.160	-0.128
Na^+	0.252	-0.340	-0.342	-0.287	0.359
NH_4^+	**-0.578**	-0.142	-0.015	0.014	0.210
Mg^{2+}	-0.051	**-0.622**	-0.096	-0.070	-0.061
K^+	0.043	-0.067	-0.048	-0.056	**-0.873**
Ca^{2+}	-0.031	**-0.654**	0.138	0.079	-0.098
BC	-0.030	0.070	**-0.905**	0.094	-0.131

The five factors reported in Table 5 were considered as corresponding to as many emission sources. Factor 1 (F1) shows high loadings for NO_3^-, SO_4^{2-}, and NH_4^+, indicating SIA as the dominant PM_{10} component, corresponding to a non-resolvable cumulative contribution from all high temperature emission sources encompassing traffic, heat and power generation, and industry (Seinfeld and Pandis, 2016). The absence of BC in this factor indicates that there is no direct link to combustion sources like those using fossil fuel. SIA is originated in secondary processes which are not directly relate to

primary sources as BC but rather reflect the regional emissions affecting a megacity due to the relatively low chemical kinetics of formation and to non-local air mass transportation (Fig. 9). Moreover, comparable patterns of concentration polar plots for SO_4^{2-} and NH_4^+ (Fig. 8) confirm their common source as well. Factor 2 (F2) associates Ca^{2+} and Mg^{2+}, indicating the mineral component of which calcium is a proxy. It represents the more abundant components in crustal materials so-called soil/road dust resuspension, derived from rock reworking, soil development, and the built environment (Lai et al., 2007). Factor 3 (F3) indicates the BC sources associated with fossil fuel combustion i.e. traffic, heating system, and industry in a megacity (Popovicheva et al., 2022). High loading only for BC in this factor suggests the absence of any strong ion relevance to combustion sources. The decoupling of BC from K^+ likely indicates that the main source of BC in the Moscow atmosphere is fossil fuel combustion while K^+ is a marker of biomass burning presenting the highest loading in Factor 5 (F5). Cl^- derived from road salt, is found alone in Factor 4 (F4). It is to note that the decoupling from Na^+ does not mean that Cl^- is not due to road salt, their association has been shown above. Relatively significant loadings of Na^+ are found both in F2 and F4. This reasonably means that, differently from chloride, which is a highly reactive mobile substance and can be degassed by atmospheric processing, the same does not hold for Na^+. Sodium is a highly conservative ion, which accumulates in the course of years in soil, where it is stabilized by ion exchange chemistry in the soil matrix to be recirculated in the lower troposphere following soil resuspension. Note that previously cited research work on the effects of DIA on soil water chemistry in Moscow revealed a decoupling of chloride ion from its cation partner Na^+, circumstance which may support the occurrence of Cl^- in factor 4 without other significant correlation.

3.3.4 Varimax analysis in summer case study: organic ions and sugars sources

For summer ion chemistry and BC are integrated by a series of chemical species including carboxylic and di-carboxylic acids, anhydrosugars (levoglucosan with its isomer mannosan), and sugars. These species were analyzed only in summer since this is the only season of high photochemistry as well as biogenic activities and biomass burning in Russia. Although it is not possible to evaluate the seasonal variation of such species, their presence in summer samples can be used to evaluate their source, also in correlation with inorganic ones. The whole dataset is subjected to an independent elaboration for receptor modelling using Varimax factor analysis (Table 6).

Table 6. Varimax loadings of the summer case-study. Bold values correspond to the most representative variables for each factor. EV stands for the explained variance, F for a factor.

	F1	F2	F3	F4	F5	F6

EV(%)	18.8	18.1	13.7	13.5	12.0	7.80
Cl^-	-0.121	**0.533**	-0.116	-0.007	-0.019	-0.080
NO_3^-	**0.453**	-0.075	-0.143	-0.006	-0.023	0.100
SO_4^{2-}	**0.497**	-0.024	-0.021	0.017	0.188	-0.047
Na^+	-0.085	-0.098	-0.260	**0.399**	0.256	0.228
NH_4^+	**0.424**	-0.095	-0.047	0.196	0.154	-0.055
Mg^{2+}	0.048	-0.020	0.059	**0.570**	-0.021	-0.039
K^+	0.030	**0.518**	-0.014	-0.053	-0.055	0.058
Ca^{2+}	0.047	0.047	0.049	**0.464**	-0.249	-0.066
BC	0.140	**0.321**	-0.064	0.125	-0.082	0.013
Oxalate	**0.454**	0.116	-0.035	-0.067	0.040	-0.096
Lactate	-0.141	0.178	**-0.544**	0.205	0.209	-0.222
Acetate	0.050	-0.035	**-0.484**	-0.218	-0.290	0.001
Formate	0.005	-0.068	**-0.548**	-0.092	-0.026	0.181
Glutarate	0.140	0.027	0.011	0.020	**-0.567**	0.074
Succinate	0.105	0.019	0.009	0.116	**-0.530**	-0.035
Levoglucosan	0.064	**0.425**	0.073	-0.122	0.090	0.039
Mannosan	0.015	-0.095	-0.085	-0.112	-0.053	**0.707**
Mannose	0.238	0.121	0.119	-0.207	0.230	0.074
Glucose	-0.024	0.246	0.164	0.238	0.077	**0.559**

Factor 1 (F1) presents high loadings of SIA and oxalates, confirming the role of photochemistry in the formation of both inorganic and organic secondary aerosols (Tsai et al., 2013). In particular, oxalates and sulfates undergo a similar chemical processing mainly associated with cloud processing (Laongsri and Harrison, 2013). Factor 2 (F2) includes Cl^-, BC, K^+, and levoglucosan. Time series of BC, nss-K, and levoglucosan in Figure S3 show a remarkably good agreement throughout the summer period. It indicates the variable influence of biomass burning which relates to large wildfires observed in the European part of Russia and particular in the region around Moscow, as shown by BWT cluster analyses (Fig. 9). It is to note that the high loading of Cl^- in F2, similar to BB markers, shows its seasonal distinct source together with a complex relationship to local origin. It means that Cl^- is contributed by two sources, i.e. road salts from which it is partially removed to the gaseous phase, and biomass burning, as was also observed by Brattich et al. (Brattich et al., 2021).

Factor 3 (F3) includes three carboxylic acids sharing similar sources. In particular, acetate is correlated with biomass burning (Tsai et al., 2013). Acetate comes mostly from primary emissions, while formate come from secondary transformations. The mass ratio of acetate and formate (A/F) is used to distinguish primary and secondary sources of these acids (Tsai et al., 2013). An A/F ratio higher than 1 indicates a prevalence of primary sources, while A/F lower than 1 indicates the contrary. In our case, the mean A/F mass ratio is 2.19, therefore the main source of these acids can be considered the urban primary sources, probably vehicular emissions (Tsai et al., 2013; Wang et al., 2007).

716 Factor 4 (F4), including Ca^{2+}, Mg^{2+}, and Na^{+}, represents the influence of road dust and soil
717 resuspension contribution thanks to the low-level turbulence and relatively drier conditions of
718 summer, capable to recirculate these components. Succinate and glutarate in Factor 5 (F5) relates to
719 oxalate and SIA as products of secondary formation from organic precursors by photochemical and
720 heterogeneous reactions (Guo et al., 2021). Factor 6 (F6) with a little influence on the overall variance
721 has a high loading of mannosan and glucose. Since mannosan is acting as biomass burning marker,
722 and glucose is the product of biogenic activity, they both reflect the co-existence of biomass burning
723 and bioaerosols which was observed in other studies (Bauer et al., 2008; Popovicheva et al., 2020).
724 High temperature in summer (Fig. S1a) definitely relates with intensive biological activities.
725 Moreover, the co-existence of sugars with anhydrosugars may be explained by suspension of soil and
726 plant debris in the heat wave of wildfires (Medeiros et al., 2006).
727
728 **3.4. Precipitation chemistry**
729 Precipitation in the form of rain and snow reflects the aerosol composition through complex in-cloud
730 and below clouds removal. The ion composition and pH are a function of the amount of condensed
731 water and the relative degree of neutralization of SIA, while pH may affect solubility of removed
732 aerosols and of those trapped in rain/snow bulk collectors (Pruppacher and Klett, 2010; Tositti et al.,
733 2018b; Vlasov et al., 2021).
734 Long-term records of precipitation chemistry at MO MSU site show the significant increase of the
735 acid precipitation number from almost absence until the level of 30% in last years (Eremina et al.,
736 2015). The percentage of acid precipitation with pH < 5 was 20.7% for a year on average, 31.0% for
737 a warm season, and only 5.7% for winter. The total ionic mineral composition does not change in
738 average, while chloride and sodium concentration were increasing.
739 Figure 2a shows precipitation events scattered throughout three seasons, they appear more abundant
740 in summer and autumn (Table S1). In the end of autumn, in December, rainfall was subsequently
741 substituted by snowfall. The pH recorded in precipitation reveals a certain tendency towards lower
742 values in spring and summer (Fig. 10), such a fact is typically recognized as pertaining to acid rains
743 (Bricker and Rice, 2003). Observed pH in spring and summer oscillate around 5-5.6.

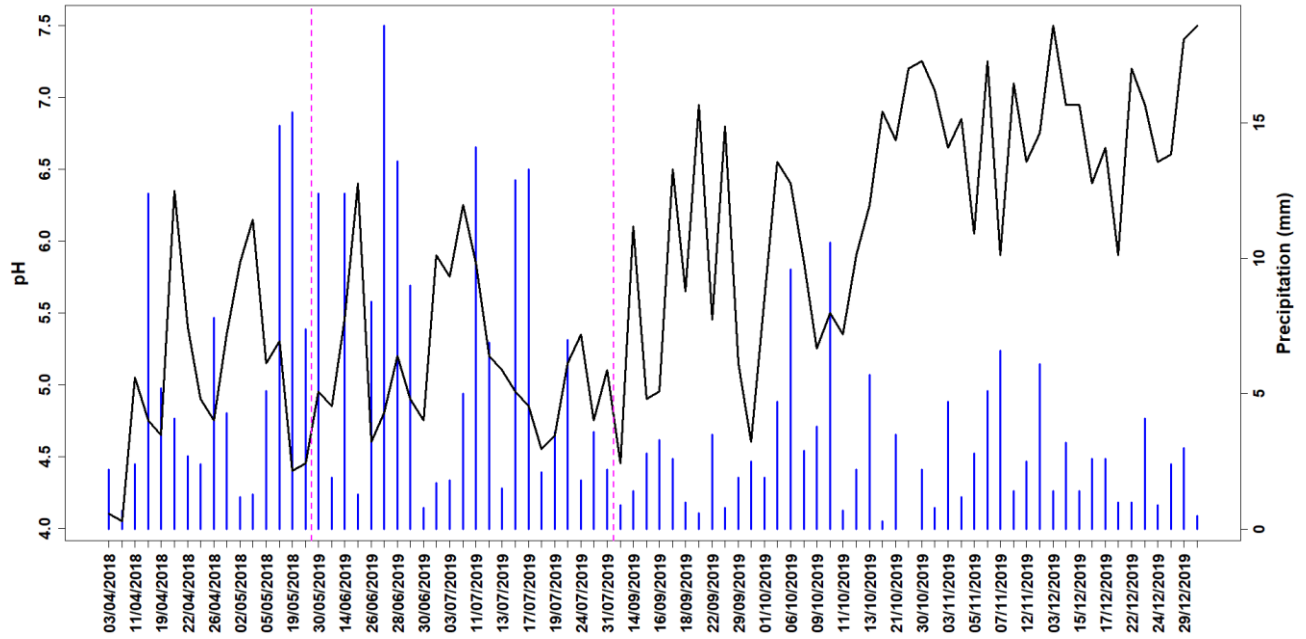

744

745 **Fig. 10**. pH (black line) and precipitation intensity (blue bars) for the whole period of study.

746

747 Since during some time in autumn soil is frozen and covered with snow at the Moscow latitude, the
748 agricultural contribution is likely negligible while traffic and industrial sources (with the support of
749 ventilation) appear to be the most important ones. These leads to scarce availability of ammonia and
750 therefore to a reduced neutralizing effect on sulfuric and nitric acids formed by SO_2 and NO_x
751 oxidation rather than to an excess of acidifying species. Increase of pH in colder seasons, above 5.6,
752 suggests both the neutralizing influence of ammonia and the contribution from carbonates in
753 resuspended alkaline urban soils (Nikiforova et al., 2017), road dust (Kasimov et al., 2019), and
754 undissolved DIAs (Korolev and Gornyakov, 2018).
755 Precipitation ion chemistry and data variability is associated with the seasonal precipitation rate as
756 well as with the type of precipitation event in terms of total volume of the deposited hydrometeor as
757 well as of the progression of the single event. Table 7 reports basic statistics for precipitation during
758 three seasons, together with pH and ion concentrations. The highest mean precipitation is observed
759 in summer while in autumn it is the lowest. The highest mean and median concentrations for almost
760 all ions were observed in spring, except HCO_3^-. Its maximum is in autumn, that is generally consistent
761 with observations in previous years according to which the average concentrations of HCO_3^- in
762 September-December are higher than in April-May (Eremina et al., 2017).

763

764 **Table 7.** Statistics of precipitation, pH, and ions concentrations (in μg L^{-1}) in three seasons.

	Spring 2018				Summer 2019				Autumn 2019			
	mean	median	min	max	mean	median	min	max	mean	median	min	max

Precipitation (mm)	5.59	4.20	0.70	15.4	6.53	4.30	0.80	18.6	2.91	2.55	0.30	10.6
pH	5.04	4.98	4.05	6.35	5.16	5.03	4.45	6.40	6.37	6.55	4.60	7.50
H^+	21.7	10.8	0.45	89.1	11.4	9.55	0.40	35.5	2.03	0.28	0.03	25.1
HCO_3^-	1.24	0.00	0.00	7.40	0.77	0.00	0.00	9.39	3.93	2.80	0.00	13.5
SO_4^{2-}	2.54	2.60	0.60	4.90	1.66	1.06	0.31	6.10	2.32	1.70	0.40	8.70
Cl^-	13.2	10.9	3.00	39.5	10.4	7.09	2.13	34.9	7.09	6.80	1.30	20.90
NO_3^{2-}	2.90	3.20	0.50	6.50	2.97	1.50	0.45	16.2	2.23	1.90	0.70	5.00
Ca^{2+}	5.96	4.50	1.10	21.0	5.03	3.45	0.68	18.9	4.29	3.70	0.80	11.0
Mg^{2+}	0.34	0.20	0.10	1.60	0.19	0.09	0.02	1.12	0.21	0.20	0.00	0.50
Na^+	1.71	1.40	0.30	4.90	0.50	0.35	0.07	1.80	0.96	0.80	0.10	2.70
K^+	0.43	0.30	0.10	2.90	0.40	0.27	0.02	2.22	0.51	0.40	0.10	3.30
NH_4^+	1.73	1.50	0.30	4.30	1.39	0.97	0.27	4.90	1.36	1.20	0.30	3.20

Spearman correlation analysis has been carried out. Based on Spearman indexes, it is found that ions pertaining to SIA appear highly correlated (> 0.70) in connection with their origin and source. Other correlations are in general lower than those observed for SIA (< 0.7), suggesting multiple sources for the other ions. An exception is represented by the ions already cited as coming from road management practices (Ca^{2+}, Mg^{2+}, and Na^+, correlations between 0.65 and 0.75). This likely reflects the influence of soil resuspension in dry periods on the precipitation chemistry, since precipitation is collected as bulk deposition, i.e. the sum of wet and dry deposition, and not with a wet only approach (Tositti et al., 2018b). Finally, H^+ and HCO_3^- appear uncorrelated in respect to all the other ions (< 0.3) and they are reciprocally anticorrelated (-0.936). This is reasonably due to the neutralizing effects of calcium and magnesium carbonates from soil resuspension acting as neutralizing agents toward H^+ which is decreased through the formation of HCO_3^-. In Moscow, during years with a deficit of acid precipitation, the predominant anion in precipitation is HCO_3^-, the source of which is carbonates of alkali and alkaline earth metals. This is confirmed by the results of thermodynamic calculations; in episodes with an excess of acids in precipitation it is associated with the absorption of ammonia from the atmosphere (Eremina et al., 2017).

Efficiency of wet removal can be appreciated analyzing simultaneously the trend of PM_{10} and precipitation, as reported in Figure 2a. Seasonal variability of scavenging ratios (ω) of SIA species (Table 9) have been calculated by taking into account the ion concentrations in aerosols, their concentrations in precipitation, and the air density, using eq.1. Scavenging ratios are determined on a seasonal basis because they have less variability compared to ones calculated using precipitation event concentrations and consider the average ion concentrations in PM_{10} during both precipitation and dry periods (Cheng and Zhang, 2017).

Table 9. Scavenging ratios calculated for SIA compounds during three seasons.

	ωNO_3^-	ωSO_4^{2-}	ωNH_4^+
Spring 2018	$7.70 \cdot 10^3$	$2.12 \cdot 10^3$	$3.17 \cdot 10^3$
Summer 2019	$3.45 \cdot 10^3$	$2.40 \cdot 10^3$	$2.70 \cdot 10^3$
Autumn 2019	$5.29 \cdot 10^3$	$3.31 \cdot 10^3$	$2.74 \cdot 10^4$

790

791 The lowest ωNO_3^- , ωNH_4^+, and ωSO_4^{2-} are determined in summer and spring, respectively. The
792 maximum ωNO_3^- is found in spring, in autumn we observe the maximum ωSO_4^{2-} and ωNH_4^+.
793 Gaseous species such as HNO_3, SO_2, and NH_3 can influence the SIA scavenging ratios since the
794 composition of the precipitation is determined by the scavenging process of both gases and particles.
795 That might be the reason of the overestimated levels of ω especially in spring and summer, when the
796 formation of SIA is favored by the photochemical reactions (Oduber et al., 2021). For instance, 88-
797 96% of NO_3^- content in rainwater is formed due to gas-phase scavenging of HNO_3, whereas 89-96%
798 of SO_4^{2-} concentration in rainwater may be due to particulate sulfate (Kasper-Giebl et al., 1999).
799 However, our findings showing ω decreasing in summer and increasing in autumn and spring are
800 consistent with estimates obtained for atmospheric air and precipitation at Canadian rural locations
801 (Cheng and Zhang, 2017).
802 Comparing the obtained values with those found in other works (Cheng and Zhang, 2017; Encinas et
803 al., 2010) the secondary ωSO_4^{2-}, ωNO_3^- and ωNH_4^+ resulted to be comparable with those calculated
804 in our study.
805 Though the scavenging ratio is widely used, it must bear in mind that its meaning and use have some
806 limitation. In fact, owing to the complexity of aerosol wet removal processes (Andronache, 2003),
807 many uncertainties in the physical meaning of the scavenging factors remain. The wet removal
808 process may indeed be split into in-cloud processes, characterized by hygroscopicity-induced
809 nucleation mechanisms, and below-cloud processes, a highly stochastic process based on the
810 impaction of droplets (snowflakes) with aerosol particles with a huge dependency on particle size.
811 Variability of ω is also influenced by a large number of factors, such as wind speed, temperature,
812 precipitation amount and type, the time elapsed between two precipitation events, nucleation
813 efficiency, vertical concentration differences, cloud type, etc. (Cheng and Zhang, 2017; Duce et al.,
814 1991; Luan et al., 2019; Oduber et al., 2021).
815

816 **4. Conclusions**

817 Characterization of ion composition together with anemological analyses sheds a light into the high
818 seasonal variability and various sources of origin, therefore add the understanding of factors
819 influencing aerosol and precipitation ion chemistry in Moscow urban background. Total inorganic
820 ions compose the biggest fraction of aerosol PM_{10} mass, up to 27% in autumn. Degree of

neutralization in summer and anions in autumn, and substantially electroneutrality in spring constraints by the season-related neutralized agents such as ammonia and carbonates. Dominance of secondary inorganic aerosols (SIA) over all the other ion species exists mostly as NH_4NO_3 and $(NH_4)_2SO_4$ in all seasons. Backward trajectories within a cluster of the prevalent air mass transportation indicate the highest regional SIA source in the northwestern direction in spring and summer. Sulfates and nitrates dominate among the SIA components, with maximum contribution of 38 and 34%, respectively, in autumn. Similarity of SO_4^{2-} and NH_4^+ relationships among the wind direction and speed reflects the significant thermodynamic stability of ammonium sulfates originated from SO_2 gas-to-particle conversion preferably in the southeast industrially developed Moscow area. High concentrations of NO_3^- are due to ground-level traffic as well as the centralized heating system operation. Salt components (Na^+ and Cl^-) are attributed to a high amount of de-icing agents used in road management. Na^+ shows a maximum in summer and minimum in autumn, with the largest variability between seasons, differently from Cl^-. While chloride is a highly reactive mobile substance and degassed by atmospheric processing, conservative potassium accumulates in soil and stabilizes by ion exchange chemistry then recirculates in the atmosphere due to soil resuspension. Chlorine depletion phenomenon follows the snow melt and demonstrates the biggest Cl^- displacing from NaCl promoted in summer by both a significant low-level turbulence and dryness, and the required HNO_3 photochemistry. Ca^{2+} and Mg^{2+} relate to local soil resuspension after snow thaw, Ca^{2+} shows an additional source from intensive building activities in the New Moscow area. Biomass burning is indicated from remote sources in the region surrounding Moscow by high K^+ concentrations in all seasons. High frequencies of backward trajectories from the European part of Russia in warm seasons confirm the large agriculture and wildfires impact to the air pollution of a megacity. Main sources of PM_{10} inorganic ions are secondary sulfates and nitrates, soil resuspension, road salt, and biomass burning in spring and autumn. Organic acid anions, K^+, and anhydrosugars detect biomass burning associated to summer wildfires. Concerning PM_{10} and ionic data there is no particularly critical issues about atmospheric pollution in Moscow urban background, in comparison to evaluated large European and Canadian cities. Lower content of SO_2^-, probably due to centralizing gas operated heating system, and comparable NO_3^- concentrations impacted by intensive traffic and industry, are found. Impact of deicing agents on Cl^- and Na^+ concentration is similar to inland cities with cold climate.

Precipitation collected in the same period shows the link between aerosol and precipitation scavenging, with increasing acidity in spring and summer. The lowest values of scavenging factor for NO_3^- and NH_4^+ was determined in summer and for SO_4^{2-} in spring, while the maximum for NO_3^-

in spring. The finding obtained can support the mitigation efforts contributing to the reduction of aerosol mass load and consequently of aerosol and precipitation acidity.

Acknowledgements

Data collection and initial treatment was funded by Russian Science Foundation, grant number 19-77-30004. Authors thank to a grant of the Ministry of Science and Higher Education of Russian Federation under the Agreement (075-15-2021-574) for data analyses support. This research was performed according to the Development program of the Interdisciplinary Scientific and Educational School of Lomonosov Moscow State University ⟪Future Planet and Global Environmental Change⟫, it was carried out using the equipment of MSU Shared Research Equipment Center "Technologies for obtaining new nanostructured materials and their complex study" which were purchased by MSU in the frame of the Equipment Renovation Program (National Project "Science"). Dr. L. Golobokova and Dr. T. Khodzher (Limnological Institute RAS) for partial performance of ion composition analyses.

References

Alastuey, A., Querol, X., Rodríguez, S., Plana, F., Lopez-Soler, A., Ruiz, C., Mantilla, E., 2004. Monitoring of atmospheric particulate matter around sources of secondary inorganic aerosol. Atmos. Environ. 38, 4979–4992. https://doi.org/10.1016/j.atmosenv.2004.06.026

Andronache, C., 2003. Estimated variability of below-cloud aerosol removal by rainfall for observed aerosol size distributions. Atmos. Chem. Phys. 3, 131–143. https://doi.org/10.5194/ACP-3-131-2003

Baklanov, A., Molina, L.T., Gauss, M., 2016. Megacities, air quality and climate. Atmos. Environ. 126, 235–249. https://doi.org/10.1016/J.ATMOSENV.2015.11.059

Bauer, H., Claeys, M., Vermeylen, R., Schueller, E., Weinke, G., Berger, A., Puxbaum, H., 2008. Arabitol and mannitol as tracers for the quantification of airborne fungal spores. Atmos. Environ. 42, 588–593. https://doi.org/10.1016/J.ATMOSENV.2007.10.013

Beccaceci, S., McGhee, E.A., Brown, R.J.C., Green, D.C., 2015. A Comparison Between a Semi-Continuous Analyzer and Filter-Based Method for Measuring Anion and Cation Concentrations in PM10 at an Urban Background Site in London. Aerosol Sci. Technol. 49, 793–801. https://doi.org/10.1080/02786826.2015.1073848

Bityukova, V.., Saulskaya, T., 2017. Changes of the anthropogenic impact of Moscow industrial zones during the recent decades. Vestn. Mosk. Unviersiteta, Seriya Geogr. 24–33.

Bityukova, V.R., Mozgunov, N.A., 2019. Spatial Features Transformation of Emission from Motor Vehicles in Moscow. Geogr. Environ. Sustain. 12, 57–73. https://doi.org/10.24057/2071-9388-2019-75

Brattich, E., Liu, H., Zhang, B., Hernández-Ceballos, M.Á., Paatero, J., Sarvan, D., Djurdjevic, V., Tositti, L., Ajtić, J., 2021. Observation and modeling of high-7Be concentration events at the surface in northern Europe associated with the instability of the Arctic polar vortex in early 2003. Atmos. Chem. Phys. 21, 17927–17951. https://doi.org/10.5194/ACP-21-17927-2021

Brattich, E., Riccio, A., Tositti, L., Cristofanelli, P., Bonasoni, P., 2015. An outstanding Saharan dust event at Mt. Cimone (2165 m a.s.l., Italy) in March 2004. Atmos. Environ. 113, 223–235. https://doi.org/10.1016/j.atmosenv.2015.05.017

Bricker, O.P., Rice, K.C., 2003. Acid Rain. Annu. Rev. Earth Planet. Sci. 21, 151–174. https://doi.org/http://dx.doi.org/10.1146/annurev.ea.21.050193.001055

Carslaw, D.C., Beevers, S.D., 2013. Characterising and understanding emission sources using

bivariate polar plots and k-means clustering. Environ. Model. Softw. 40, 325–329. https://doi.org/10.1016/j.envsoft.2012.09.005

Carslaw, D.C., Ropkins, K., 2012. Openair - An r package for air quality data analysis. Environ. Model. Softw. 27–28, 52–61. https://doi.org/10.1016/j.envsoft.2011.09.008

Cheng, I., Zhang, L., 2017. Long-term air concentrations, wet deposition, and scavenging ratios of inorganic ions, HNO3, and SO2 and assessment of aerosol and precipitation acidity at Canadian rural locations. Atmos. Chem. Phys. 17, 4711–4730. https://doi.org/10.5194/ACP-17-4711-2017

Chow, J., Lowenthal, D.H.., Antony Chen, L.., Wang, X., Watson, J.G., 2015. Mass reconstruction methods for PM2.5: a review. Air Qual. Atmos. Heal. 8, 243–263. https://doi.org/10.1007/s11869-015-0338-3

Chubarova, N.E., Nezval', E.I., Belikov, I.B., Gorbarenko, E. V., Eremina, I.D., Zhdanova, E.Y., Korneva, I.A., Konstantinov, P.I., Lokoshchenko, M.A., Skorokhod, A.I., Shilovtseva, O.A., 2014. Climatic and environmental characteristics of Moscow megalopolis according to the data of the Moscow State University Meteorological Observatory over 60 years. Russ. Meteorol. Hydrol. 39, 602–613. https://doi.org/10.3103/S1068373914090052

Cui, L., Song, X., Zhong, G., 2021. Comparative analysis of three methods for hysplit atmospheric trajectories clustering. Atmosphere (Basel). 12, 698. https://doi.org/10.3390/ATMOS12060698

Dadashazar, H., Ma, L., Sorooshian, A., 2019. Sources of pollution and interrelationships between aerosol and precipitation chemistry at a central California site. Sci. Total Environ. 651, 1776–1787. https://doi.org/10.1016/j.scitotenv.2018.10.086

Diapouli, E., Kalogridis, A.C., Markantonaki, C., Vratolis, S., Fetfatzis, P., Colombi, C., Eleftheriadis, K., 2017. Annual Variability of Black Carbon Concentrations Originating from Biomass and Fossil Fuel Combustion for the Suburban Aerosol in Athens, Greece. Atmosphere (Basel). 8, 234. https://doi.org/10.3390/ATMOS8120234

Duce, R.A., Liss, P.S., Merrill, J.T., Atlas, E.L., Buat- Menard, P., Hicks, B.B., Miller, J.M., Prospero, J.M., Arimoto, R., Church, T.M., Ellis, W., Galloway, J.N., Hansen, L., Jickells, T.D., Knap, A.H., Reinhardt, K.H., Schneider, B., Soudine, A., Tokos, J.J., Tsunogai, S., Wollast, R., Zhou, M., 1991. The atmospheric input of trace species to the world ocean. Global Biogeochem. Cycles 5, 193–259. https://doi.org/10.1029/91GB01778

Elansky, N., 2014. Air quality and CO emissions in the Moscow megacity. Urban Clim. 8, 42–56.

https://doi.org/10.1016/j.uclim.2014.01.007

Elansky, N.F., Lavrova, O.V., Rakin, A.A., Skorokhod, A.I., 2014. Anthropogenic disturbances of the atmosphere in Moscow region. Dokl. Earth Sci. 454, 158–162. https://doi.org/10.1134/S1028334X14020020

Elansky, N.F., Lokoshchenko, M.A., Belikov, I.B., Skorokhod, A.I., Shumskii, R.A., 2007. Variability of trace gases in the atmospheric surface layer from observations in the city of Moscow. Izv. - Atmos. Ocean Phys. 43, 219–231. https://doi.org/10.1134/S0001433807020089

Elansky, N.F., Ponomarev, N.A., Verevkin, Y.M., 2018. Air quality and pollutant emissions in the Moscow megacity in 2005–2014. Atmos. Environ. 175, 54–64. https://doi.org/10.1016/j.atmosenv.2017.11.057

Encinas, D., Calzada, I., Casado, H., 2010. Scavenging Ratios in an Urban Area in the Spanish Basque Country. Aerosol Sci. Technol. 38, 685–691. https://doi.org/http://dx.doi.org/10.1080/02786820490460716

Engelmann, R.J., 1971. Scavenging Prediction Using Ratios of Concentrations in Air and Precipitation in: Journal of Applied Meteorology and Climatology Volume 10 Issue 3 (1971). J. Appl. Meteorol. Climatol. 10, 493–497. https://doi.org/https://doi.org/10.1175/1520-0450(1971)010<0493:SPUROC>2.0.CO;2

Eremina, I.D., 2019. Chemical composition of atmospheric precipitation in Moscow and the trends of its long-term changes | Eremina | Vestnik Moskovskogo universiteta. Seriya 5, Geografiya. Vestn. Mosk. Unviersiteta, Seriya Geogr. 3–10.

Eremina, I.D., Aloyan, A.E., Arutyunyan, V.O., Larin, I.K., Chubarova, N.E., Yermakov, A.N., 2017. Hydrocarbonates in atmospheric precipitation of Moscow: Monitoring data and analysis. Izv. Atmos. Ocean. Phys. 53, 334–342. https://doi.org/10.1134/S0001433817030069

Eremina, I.D., Aloyan, A.E., Arutyunyan, V.O., Larin, I.K., Chubarova, N.E., Yermakov, A.N., 2015. Acidity and mineral composition of precipitation in Moscow: Influence of deicing salts. Izv. - Atmos. Ocean Phys. 51, 624–632. https://doi.org/10.1134/S0001433815050047

Eremina, I.D., Vasil'chuk, J.Y., 2019. Temporal Variations in Chemical Composition of Snow Cover in Moscow. Geogr. Environ. Sustain. 12, 148–158. https://doi.org/10.24057/2071-9388-2019-79

Finardi, S., Silibello, C., D'Allura, A., Radice, P., 2014. Analysis of pollutants exchange between the Po Valley and the surrounding European region. Urban Clim. 10, 682–702.

https://doi.org/10.1016/J.UCLIM.2014.02.002

Finlayson-Pitts, B.J.., Pitts, J.N., 2000. Chemistry of the Upper and Lower Atmosphere: Theory, Experiments, and Applications, First Ed. ed. Academic Press, San Diego, CA. https://doi.org/https://doi.org/10.1016/B978-0-12-257060-5.X5000-X

Font, A., Guiseppin, L., Blangiardo, M., Ghersi, V., Fuller, G.W., 2019. A tale of two cities: is air pollution improving in Paris and London? Environ. Pollut. 249, 1–12. https://doi.org/10.1016/J.ENVPOL.2019.01.040

Fountoukis, C., Nenes, A., 2007. ISORROPIAII: A computationally efficient thermodynamic equilibrium model for K+-Ca2+-Mg2+-NH4+-Na+-SO42--NO3--Cl--H2O aerosols. Atmos. Chem. Phys. 7, 4639–4659. https://doi.org/10.5194/acp-7-4639-2007

Fuzzi, S., Baltensperger, U., Carslaw, K., Decesari, S., Denier Van Der Gon, H., Facchini, M.C., Fowler, D., Koren, I., Langford, B., Lohmann, U., Nemitz, E., Pandis, S., Riipinen, I., Rudich, Y., Schaap, M., Slowik, J.G., Spracklen, D. V., Vignati, E., Wild, M., Williams, M., Gilardoni, S., 2015. Particulate matter, air quality and climate: Lessons learned and future needs. Atmos. Chem. Phys. 15, 8217–8299. https://doi.org/10.5194/ACP-15-8217-2015

Gentner, D.R., Jathar, S.H., Gordon, T.D., Bahreini, R., Day, D.A., El Haddad, I., Hayes, P.L., Pieber, S.M., Platt, S.M., De Gouw, J., Goldstein, A.H., Harley, R.A., Jimenez, J.L., Prévôt, A.S.H., Robinson, A.L., 2017. Review of Urban Secondary Organic Aerosol Formation from Gasoline and Diesel Motor Vehicle Emissions. Environ. Sci. Technol. 51, 1074–1093. https://doi.org/10.1021/ACS.EST.6B04509/SUPPL_FILE/ES6B04509_SI_001.PDF

Golitsyn, G.S., Grechko, E.I., Wang, G., Wang, P., Dzhola, A. V., Emilenko, A.S., Kopeikin, V.M., Rakitin, V.S., Safronov, A.N., Fokeeva, E. V., 2015. Studying the pollution of Moscow and Beijing atmospheres with carbon monoxide and aerosol. Izv. - Atmos. Ocean Phys. 51, 1–11. https://doi.org/10.1134/S0001433815010041

Golobokova, L., Khodzher, T., Khuriganova, O., Marinayte, I., Onishchuk, N., Rusanova, P., Potemkin, V., 2020. Variability of chemical properties of the atmospheric aerosol above lake baikal during large wildfires in siberia. Atmosphere (Basel). 11, 1–21. https://doi.org/10.3390/atmos11111230

Guo, W., Zhang, X., Zhang, Z., Zheng, N., Xiao, Hongwei, Xiao, Huayun, 2021. Low-molecular-weight carboxylates in urban southwestern China: Source identification and effects on aerosol acidity. Atmos. Pollut. Res. 12, 101141. https://doi.org/10.1016/J.APR.2021.101141

Hama, S.M.L., Cordell, R.L., Staelens, J., Mooibroek, D., Monks, P.S., 2018. Chemical composition and source identification of PM10 in five North Western European cities. Atmos. Res. 214, 135–149. https://doi.org/10.1016/J.ATMOSRES.2018.07.014

Heal, M.R., Kumar, P., Harrison, R.M., 2012. Particles, air quality, policy and health. Chem. Soc. Rev. 41, 6606–6630. https://doi.org/10.1039/c2cs35076a

Hewitt, C.N., 2001. The atmospheric chemistry of sulphur and nitrogen in power station plumes. Atmos. Environ. https://doi.org/10.1016/S1352-2310(00)00463-5

Hoffman, R.C., Laskin, A., Finlayson-Pitts, B.J., 2004. Sodium nitrate particles: physical and chemical properties during hydration and dehydration, and implications for aged sea salt aerosols. J. Aerosol Sci. 35, 869–887. https://doi.org/10.1016/J.JAEROSCI.2004.02.003

Hopke, P.K., 2016. Review of receptor modeling methods for source apportionment. J. Air Waste Manag. Assoc. https://doi.org/10.1080/10962247.2016.1140693

Hristova, E., Veleva, B., Georgieva, E., Branzov, H., 2020. Application of Positive Matrix Factorization Receptor Model for Source Identification of PM10 in the City of Sofia, Bulgaria. Atmos. 2020, Vol. 11, Page 890 11, 890. https://doi.org/10.3390/ATMOS11090890

Jeong, C.H., Traub, A., Huang, A., Hilker, N., Wang, J.M., Herod, D., Dabek-Zlotorzynska, E., Celo, V., Evans, G.J., 2020. Long-term analysis of PM2.5 from 2004 to 2017 in Toronto: Composition, sources, and oxidative potential. Environ. Pollut. 263, 114652. https://doi.org/10.1016/J.ENVPOL.2020.114652

Karydis, V., Tsimpidi, A., Pozzer, A., Lelieveld, J., 2020. How alkaline compounds control atmospheric aerosol acidity. Atmos. Chem. Phys. 2018, 1–22. https://doi.org/10.5194/acp-2020-1222

Kasimov, N.S., Kosheleva, N.E., Vlasov, D. V., Nabelkina, K.S., Ryzhov, A. V., 2019. Physicochemical Properties of Road Dust in Moscow. Geogr. Environ. Sustain. 12, 96–113. https://doi.org/10.24057/2071-9388-2019-55

Kasper-Giebl, A., Kalina, M.F., Puxbaum, H., 1999. Scavenging ratios for sulfate, ammonium and nitrate determined at Mt. Sonnblick (3106 m a.s.l.). Atmos. Environ. 33, 895–906. https://doi.org/10.1016/S1352-2310(98)00279-9

Kawamura, K., Bikkina, S., 2016. A review of dicarboxylic acids and related compounds in atmospheric aerosols: Molecular distributions, sources and transformation. Atmos. Res. https://doi.org/10.1016/j.atmosres.2015.11.018

Koçak, M., Mihalopoulos, N., Kubilay, N., 2007. Chemical composition of the fine and coarse fraction of aerosols in the northeastern Mediterranean. Atmos. Environ. 41, 7351–7368. https://doi.org/10.1016/j.atmosenv.2007.05.011

Kolesar, K.R., Mattson, C.N., Peterson, P.K., May, N.W., Prendergast, R.K., Pratt, K.A., 2018. Increases in wintertime PM2.5 sodium and chloride linked to snowfall and road salt application. Atmos. Environ. 177, 195–202. https://doi.org/10.1016/J.ATMOSENV.2018.01.008

Korolev, V.A., Gornyakov, A.K., 2018. Impact assessment of the anti-icing reagents application when conducting engineereing-ecological surveys in cities. Eng. Surv. 1, 66–78. https://doi.org/https://doi.org/10.25296/1997-8650-2018-1-2-66-78

Kosheleva, N.E., Dorokhova, M.F., Kuzminskaya, N.Y., Ryzhov, A.V., Kasimov, N.S., 2018. Impact of motor vehicles on the ecological state of soils in the western district of Moscow. Moscow Univ. Bull. Ser. 5. Geogr. 2, 16–27.

Kotowski, T., Motyka, J., Knap, W., Bielewski, J., 2020. 17-Year study on the chemical composition of rain, snow and sleet in very dusty air (Krakow, Poland). J. Hydrol. 582, 124543. https://doi.org/10.1016/J.JHYDROL.2020.124543

Kul'bachevskii, A.O., 2021. Report on the state of the environment in Moscow in 2020 [WWW Document]. Dep. Nat. Environ. Prot. Moscow Gov. URL https://www.akm.ru/eng/press/state-report-on-the-state-and-environmental-protection-in-russia-in-2020/ (accessed 1.27.22).

Lai, S. chao, Zou, S. chun, Cao, J. ji, Lee, S. cheng, Ho, K. fai, 2007. Characterizing ionic species in PM2.5 and PM10 in four Pearl River Delta cities, South China. J. Environ. Sci. 19, 939–947. https://doi.org/10.1016/S1001-0742(07)60155-7

Laongsri, B., Harrison, R.M., 2013. Atmospheric behaviour of particulate oxalate at UK urban background and rural sites. Atmos. Environ. 71, 319–326. https://doi.org/10.1016/j.atmosenv.2013.02.015

Luan, T., Guo, X., Zhang, T., Guo, L., 2019. Below-Cloud Aerosol Scavenging by Different-Intensity Rains in Beijing City. J. Meteorol. Res. 2019 331 33, 126–137. https://doi.org/10.1007/S13351-019-8079-0

Mann, H.B., Whitney, D.R., 1947. On a Test of Whether one of Two Random Variables is Stochastically Larger than the Other. Ann. Math. Stat. 18, 50–60. https://doi.org/https://doi.org/10.1214/aoms/1177730491

McNamara, S.M., Kolesar, K.R., Wang, S., Kirpes, R.M., May, N.W., Gunsch, M.J., Cook, R.D.,

Fuentes, J.D., Hornbrook, R.S., Apel, E.C., China, S., Laskin, A., Pratt, K.A., 2020. Observation of Road Salt Aerosol Driving Inland Wintertime Atmospheric Chlorine Chemistry. ACS Cent. Sci. 6, 684–694. https://doi.org/10.1021/ACSCENTSCI.9B00994

Medeiros, P.M., Conte, M.H., Weber, J.C., Simoneit, B.R.T., 2006. Sugars as source indicators of biogenic organic carbon in aerosols collected above the Howland Experimental Forest, Maine. Atmos. Environ. 40, 1694–1705. https://doi.org/10.1016/J.ATMOSENV.2005.11.001

Morozzi, P., Bolelli, L., Brattich, E., Ferri, E.N., Girotti, S., Sangiorgi, S., Orza, J.A.G., Piñero-García, F., Tositti, L., 2021. Chemiluminescent fingerprints from airborne particulate matter: A luminol-based assay for the characterization of oxidative potential with kinetical implications. Sci. Total Environ. 789, 148005. https://doi.org/10.1016/J.SCITOTENV.2021.148005

Nava, S., Lucarelli, F., Amato, F., Becagli, S., Calzolai, G., Chiari, M., Giannoni, M., Traversi, R., Udisti, R., 2015. Biomass burning contributions estimated by synergistic coupling of daily and hourly aerosol composition records. Sci. Total Environ. 511, 11–20. https://doi.org/10.1016/J.SCITOTENV.2014.11.034

Nikiforova, E.M., Kasimov, N.S., Kosheleva, N.E., 2017. Long-term dynamics of anthropogenic solonetzicity in soils of the Eastern okrug of Moscow under the impact of deicing salts. Eurasian Soil Sci. 50, 84–94. https://doi.org/10.1134/S1064229317010100

Nikiforova, E.M., Kasimov, N.S., Kosheleva, N.E., 2014. Long-term dynamics of the anthropogenic salinization of soils in Moscow (by the example of the Eastern district). Eurasian Soil Sci. 47, 203–215. https://doi.org/10.1134/S1064229314030041

Oduber, F., Calvo, A.I., Blanco-Alegre, C., Castro, A., Alves, C., Cerqueira, M., Lucarelli, F., Nava, S., Calzolai, G., Martin-Villacorta, J., Esteves, V., Fraile, R., 2021. Towards a model for aerosol removal by rain scavenging: The role of physical-chemical characteristics of raindrops. Water Res. 190, 116758. https://doi.org/10.1016/J.WATRES.2020.116758

Ott, W.R., 1990. A physical explanation of the lognormality of pollutant concentrations. J. Air Waste Manage. Assoc. 40, 1378–1383. https://doi.org/10.1080/10473289.1990.10466789

Pavuluri, C.M., Kawamura, K., Swaminathan, T., 2010. Water-soluble organic carbon, dicarboxylic acids, ketoacids, and α-dicarbonyls in the tropical Indian aerosols. J. Geophys. Res. Atmos. 115, D11302. https://doi.org/10.1029/2009JD012661

Perrone, M.G., Vratolis, S., Georgieva, E., Török, S., Šega, K., Veleva, B., Osán, J., Bešlić, I., Kertész, Z., Pernigotti, D., Eleftheriadis, K., Belis, C.A., 2018. Sources and geographic origin

of particulate matter in urban areas of the Danube macro-region: The cases of Zagreb (Croatia), Budapest (Hungary) and Sofia (Bulgaria). Sci. Total Environ. 619–620, 1515–1529. https://doi.org/10.1016/J.SCITOTENV.2017.11.092

Pio, C.A., Silva, P.A., Cerqueira, M.A., Nunes, T. V., 2005. Diurnal and seasonal emissions of volatile organic compounds from cork oak (Quercus suber) trees. Atmos. Environ. 39, 1817–1827. https://doi.org/10.1016/j.atmosenv.2004.11.018

Popovicheva, O., Chichaeva, M., Kobelev, V., Sinitskiy, A., Hansen, A., 2020a. Black Carbon in urban emissions on the Polar Circle, in: 26th International Symposium on Atmospheric and Ocean Optics, Atmospheric Physics. SPIE-Intl Soc Optical Eng, p. 344. https://doi.org/10.1117/12.2577550

Popovicheva, O., Chichaeva, M., Kovach, R., Zhdanova, E., Kasimov, N., 2022. Seasonal, Weekly, and Diurnal Black Carbon in Moscow Megacity Background under Impact of Urban and Regional Sources. Atmosphere (Basel). 13, 563. https://doi.org/10.3390/ATMOS13040563

Popovicheva, O., Ivanov, A., Vojtisek, M., 2020b. Functional Factors of Biomass Burning Contribution to Spring Aerosol Composition in a Megacity: Combined FTIR-PCA Analyses. Atmosphere (Basel). 11, 319. https://doi.org/https://doi.org/10.3390/atmos11040319

Popovicheva, O., Kistler, M., Kireeva, E., Persiantseva, N., Timofeev, M., Kopeikin, V., Kasper-Giebl, A., 2014. Physicochemical characterization of smoke aerosol during large-scale wildfires: Extreme event of August 2010 in Moscow. Atmos. Environ. 96, 405–414.

Popovicheva, O., Padoan, S., Schnelle-Kreis, J., Nguyen, D.-L., Adam, T., Kistler, M., Steinkogler, T., Kasper-Giebl, A., Zimmerman, R., Chubarova, N., 2020c. Spring aerosol in urban atmosphere of megacity: analytical and statistical assessment for source impacts. Aerosol Air Qual. Res. 20. https://doi.org/10.4209/aaqr.2019.08.0412

Popovicheva, O., Volpert, E., Sitnikov, N.M., Chichaeva, M.A., Padoan, S., 2020d. Black carbon in spring aerosols of Moscow urban background. Geogr. Environ. Sustain. 13, 233–243. https://doi.org/10.24057/2071-9388-2019-90

Pöschl, U., 2005. Atmospheric aerosols: Composition, transformation, climate and health effects. Angew. Chemie - Int. Ed. 44, 7520–7540. https://doi.org/10.1002/anie.200501122

Pöschl, U., Shiraiwa, M., 2015. Multiphase Chemistry at the Atmosphere-Biosphere Interface Influencing Climate and Public Health in the Anthropocene. Chem. Rev. 115, 4440–4475. https://doi.org/10.1021/cr500487s

Prinn, R.G., 2003. The Cleansing Capacity of the Atmosphere. Annu. Rev. Environ. Resour. 28, 29–57. https://doi.org/https://doi.org/10.1146/annurev.energy.28.011503.163425

Pruppacher, H.R., Klett, J.D., 2010. Microphysics of Clouds and Precipitation, Atmospheric and Oceanographic Sciences Library. Springer Netherlands, Dordrecht. https://doi.org/10.1007/978-0-306-48100-0

Putaud, J.P., Van Dingenen, R., Alastuey, A., Bauer, H., Birmili, W., Cyrys, J., Flentje, H., Fuzzi, S., Gehrig, R., Hansson, H.C., Harrison, R.M., Herrmann, H., Hitzenberger, R., Hüglin, C., Jones, A.M., Kasper-Giebl, A., Kiss, G., Kousa, A., Kuhlbusch, T.A.J., Löschau, G., Maenhaut, W., Molnar, A., Moreno, T., Pekkanen, J., Perrino, C., Pitz, M., Puxbaum, H., Querol, X., Rodriguez, S., Salma, I., Schwarz, J., Smolik, J., Schneider, J., Spindler, G., ten Brink, H., Tursic, J., Viana, M., Wiedensohler, A., Raes, F., 2010. A European aerosol phenomenology - 3: Physical and chemical characteristics of particulate matter from 60 rural, urban, and kerbside sites across Europe. Atmos. Environ. 44, 1308–1320. https://doi.org/10.1016/j.atmosenv.2009.12.011

Raes, F., Van Dingenen, R., Vignati, E., Wilson, J., Putaud, J.-P., Seinfeld, J.H., Adams, P., 2000. Formation and cycling of aerosols in the global troposphere. Atmos. Environ. https://doi.org/10.1016/S1352-2310(00)00239-9

Saraga, D., Maggos, T., Degrendele, C., Klánová, J., Horvat, M., Kocman, D., Kanduč, T., Garcia Dos Santos, S., Franco, R., Gómez, P.M., Manousakas, M., Bairachtari, K., Eleftheriadis, K., Kermenidou, M., Karakitsios, S., Gotti, A., Sarigiannis, D., 2021. Multi-city comparative PM2.5 source apportionment for fifteen sites in Europe: The ICARUS project. Sci. Total Environ. 751, 141855. https://doi.org/10.1016/j.scitotenv.2020.141855

Schauer, J.J., Kleeman, M.J., Cass, G.R., Simoneit, B.R.T., 2002. Measurement of emissions from air pollution sources. 5. C1 - C32 organic compounds from gasoline-powered motor vehicles. Environ. Sci. Technol. 36, 1169–1180. https://doi.org/10.1021/es0108077

Schwarz, J., Pokorná, P., Rychlík, Š., Škáchová, H., Vlček, O., Smolík, J., Ždímal, V., Hůnová, I., 2019. Assessment of air pollution origin based on year-long parallel measurement of PM2.5 and PM10 at two suburban sites in Prague, Czech Republic. Sci. Total Environ. 664, 1107–1116. https://doi.org/10.1016/J.SCITOTENV.2019.01.426

Seinfeld, J.H.., Pandis, S.N., 2016. Atmospheric Chemistry and Physics: From Air Pollution to Climate Change, Environment: Science and Policy for Sustainable Development. https://doi.org/10.1080/00139157.1999.10544295

Seinfeld, J.H., Pandis, S.N., 1998. Chemistry of the atmospheric aqueous phase. Atmos. Chem. Phys.

From Air Pollut. to Clim. Chang. 337407.

Spearman, C., 2010. The Proof and Measurement of Association between Two Things. Int. J. Epidemiol. 39, 1137–1150. https://doi.org/https://doi.org/10.1093/ije/dyq191

Srivastava, D., Favez, O., Bonnaire, N., Lucarelli, F., Haeffelin, M., Perraudin, E., Gros, V., Villenave, E., Albinet, A., 2018. Speciation of organic fractions does matter for aerosol source apportionment. Part 2: Intensive short-term campaign in the Paris area (France). Sci. Total Environ. 634, 267–278. https://doi.org/10.1016/J.SCITOTENV.2018.03.296

Stein, A.F., Draxler, R.R., Rolph, G.D., Stunder, B.J.B., Cohen, M.D., Ngan, F., 2015. Noaa's hysplit atmospheric transport and dispersion modeling system. Bull. Am. Meteorol. Soc. 96, 2059–2077. https://doi.org/10.1175/BAMS-D-14-00110.1

Stieger, B., Spindler, G., Fahlbusch, B., Müller, K., Grüner, A., Poulain, L., Thöni, L., Seitler, E., Wallasch, M., Herrmann, H., 2018. Measurements of PM10 ions and trace gases with the online system MARGA at the research station Melpitz in Germany – A five-year study. J. Atmos. Chem. 75, 33–70. https://doi.org/10.1007/S10874-017-9361-0

Tang, L., Haeger-Eugensson, M., Sjöberg, K., Wichmann, J., Molnár, P., Sallsten, G., 2014. Estimation of the long-range transport contribution from secondary inorganic components to urban background PM10 concentrations in south-western Sweden during 1986-2010. Atmos. Environ. 89, 93–101. https://doi.org/10.1016/J.ATMOSENV.2014.02.018

Tositti, L., 2018. The relationship between health effects and airborne particulate constituents, in: Clinical Handbook of Air Pollution-Related Diseases. Springer International Publishing, pp. 33–54. https://doi.org/10.1007/978-3-319-62731-1_3

Tositti, L., Brattich, E., Cassardo, C., Morozzi, P., Bracci, A., Marinoni, A., Di Sabatino, S., Porcù, F., Zappi, A., 2021. Development and evolution of an anomalous Asian dust event across Europe in March 2020. Atmos. Chem. Phys. Discuss. 1–39. https://doi.org/10.5194/ACP-2021-429

Tositti, L., Brattich, E., Masiol, M., Baldacci, D., Ceccato, D., Parmeggiani, S., Stracquadanio, M., Zappoli, S., 2014. Source apportionment of particulate matter in a large city of southeastern Po Valley (Bologna, Italy). Environ. Sci. Pollut. Res. 21, 872–890. https://doi.org/10.1007/s11356-013-1911-7

Tositti, L., Brattich, E., Parmeggiani, S., Bolelli, L., Ferri, E., Girotti, S., 2018a. Airborne particulate matter biotoxicity estimated by chemometric analysis on bacterial luminescence data. Sci. Total Environ. 640–641, 1512–1520. https://doi.org/10.1016/J.SCITOTENV.2018.06.024

Tositti, L., Pieri, L., Brattich, E., Parmeggiani, S., Ventura, F., 2018b. Chemical characteristics of atmospheric bulk deposition in a semi-rural area of the Po Valley (Italy). J. Atmos. Chem. 75, 97–121. https://doi.org/10.1007/s10874-017-9365-9

Tsai, Y.I., Kuo, S.C., 2013. Contributions of low molecular weight carboxylic acids to aerosols and wet deposition in a natural subtropical broad-leaved forest environment. Atmos. Environ. 81, 270–279. https://doi.org/10.1016/j.atmosenv.2013.08.061

Tsai, Y.I., Sopajaree, K., Chotruksa, A., Wu, H.C., Kuo, S.C., 2013. Source indicators of biomass burning associated with inorganic salts and carboxylates in dry season ambient aerosol in Chiang Mai Basin, Thailand. Atmos. Environ. 78, 93–104. https://doi.org/10.1016/J.ATMOSENV.2012.09.040

Van Espen, P., Adams, F., 1983. The application of principal component and factor analysis procedures to data for element concentrations in aerosols from a remote region. Anal. Chim. Acta 150, 153–161. https://doi.org/10.1016/S0003-2670(00)85467-7

Vet, R., Artz, R.S., Carou, S., Shaw, M., Ro, C.U., Aas, W., Baker, A., Bowersox, V.C., Dentener, F., Galy-Lacaux, C., Hou, A., Pienaar, J.J., Gillett, R., Forti, M.C., Gromov, S., Hara, H., Khodzher, T., Mahowald, N.M., Nickovic, S., Rao, P.S.P., Reid, N.W., 2014. A global assessment of precipitation chemistry and deposition of sulfur, nitrogen, sea salt, base cations, organic acids, acidity and pH, and phosphorus. Atmos. Environ. 93, 3–100. https://doi.org/10.1016/j.atmosenv.2013.10.060

Vlasov, D., Kosheleva, N., Kasimov, N., 2021. Spatial distribution and sources of potentially toxic elements in road dust and its PM10 fraction of Moscow megacity. Sci. Total Environ. 761. https://doi.org/10.1016/j.scitotenv.2020.143267

Vuorenmaa, J., Augustaitis, A., Beudert, B., Bochenek, W., Clarke, N., de Wit, H.A., Dirnböck, T., Frey, J., Hakola, H., Kleemola, S., Kobler, J., Krám, P., Lindroos, A.J., Lundin, L., Löfgren, S., Marchetto, A., Pecka, T., Schulte-Bisping, H., Skotak, K., Srybny, A., Szpikowski, J., Ukonmaanaho, L., Váňa, M., Åkerblom, S., Forsius, M., 2018. Long-term changes (1990–2015) in the atmospheric deposition and runoff water chemistry of sulphate, inorganic nitrogen and acidity for forested catchments in Europe in relation to changes in emissions and hydrometeorological conditions. Sci. Total Environ. 625, 1129–1145. https://doi.org/10.1016/j.scitotenv.2017.12.245

Wang, G., Kawamura, K., Lee, S., Ho, K., Cao, J., 2006. Molecular, seasonal and spatial distributions of organic aerosols from fourteen Chinese cities. Environ. Sci. Technol. 40, 4619–4625.

https://doi.org/10.1021/es060291x

Wang, Y., Zhuang, G., Chen, S., An, Z., Zheng, A., 2007. Characteristics and sources of formic, acetic and oxalic acids in PM2.5 and PM10 aerosols in Beijing, China. Atmos. Res. 84, 169–181. https://doi.org/10.1016/J.ATMOSRES.2006.07.001

WHO, 2013. Health effects of particulate matter. Policy implications for countries in eastern Europe, Caucasus and central Asia (2013).

Wieprecht, W., Lutz, M., John, A., Lüdtke, C., Möller, D., Acker, K., 2004. PM10 Aerosol mass and composition in and around Berlin (Germany). J. Aerosol Sci. 35, 453–464. https://doi.org/10.1016/J.JAEROSCI.2004.06.028

Yang, L., Yu, L.E., 2008. Measurements of oxalic acid, oxalates, malonic acid, and malonates in atmospheric particulates. Environ. Sci. Technol. 42, 9268–9275. https://doi.org/10.1021/es801820z

Reviewer #1: Comments on the manuscript "Factors influencing aerosol and precipitation ion chemistry in urban background of northern megacity"
The revised manuscript has made some responses to my previous concerns. It is clear that the authors have taken our comments seriously and have provided new information, clarifications, and new lines of evidence that help support their claim. Also, it seems to me too that the conclusions of the paper might well be supported by the observations. However, there are still some minor comments that need to be addressed.

Line 354: The high PM10 concentration in spring is mainly caused by the deposition of terrestrial crustal weathering materials. So, where do these natural particulate materials mainly come from? Whether there are arid areas around the study area? And the natural environment around the study area needs to be introduced in this manuscript.

As for the crustal component the spring contribution seems to be significantly contributed by the road salt which includes a mineral insoluble fraction up to 20 % by weight beside saline compounds, added to promote friction over ice. Towards the end of spring following ice melt, it may become easily available for resuspension, together with the soil component from the surrounding area around the sampling station.

Line 401: In this part, the authors compared and analyzed the physicochemical composition of aerosols between the study area and other European cities. I suggest that the author add a few sentences to summarize the level of atmospheric environment in Moscow compared with these cities, for example, serious, moderate or light pollution.

The data presented in this work have pros and cons. Pros refer to its novelty, since it concerns a location so far limitedly investigated for its air quality, despite its utmost importance.
Cons refer to the relatively low number of samples analyzed, limiting deductions and environmental diagnosis to the period concerned.
Although a longer sampling campaign would be required to draw conclusive considerations, our data indicate that the pollution in Moscow is comparable, if not lower, than that of also smaller cities. Paris and London, moreover, have significative higher pollution, but with certainly lower dimensions and populations.

Lines 541-542: Why do these two substances exist in all seasons?

While nitrates are well known combustion byproducts of secondary origin, the origin of ammonia, gaseous precursor of nitrate counter-cation as a result of HNO3 neutralization in the troposphere, are known to be agricultural activities, industrial chemosynthesis, especially for fertilizer production and vehicle catalytic converters due to excess NO reduction. The latter source is a potentially significant source across Moscow megacity throughout the year given the importance of vehicular traffic as a pollution source which can therefore compare to the expected seasonality of the former contribution, which is in turn affected by mesoscale to regional transportation

Line 551: The authors determined the seasonal source of aerosol in the study area based on wind direction and backward airmass trajectory during the traceability analysis of atmospheric materials. It would be nice to add a description of potential source areas.

As already stated, we suppose that most of the observed pollution is due to urban activities, and in this sense, we already described the surroundings of the sampling site (e.g.: Figure 1) with the industrial facilities location and the highway network near the Moscow State University where the sampling station is operated. The two most important and to some extent peculiar pollution sources are those emitted by wildfires in the area surrounding Moscow, already described at the end of paragraph 3.3.1, and by the resuspension of road salt used for traffic management, which is clearly described along the text. Therefore, we decided not to further modify the text.

Line 723: In this study, the authors analyzed the seasonal variation in the concentrations of various ions and BC of aerosol and precipitation, and traced their provenance by using wind direction distribution and backward air mass trajectory. However, the seasonal differences of target substances in aerosols and precipitation have not been systematically expounded. These two environmental media retain information on dry and wet deposition, and it is important to understand the differences in their chemical compositions for further understanding the different atmospheric deposition mechanisms.

In the absence of a wet and dry sampler, it is hard to discriminate and characterize accurately deposition processes, which can be further biased by the influence of local soil resuspension. All these factors have been explained accurately, including some comments concerning the difficulties in associating the origin of aerosols from which precipitation may form with local aerosols. In fact, one of the main unresolved problems in the understanding of wet scavenging mechanisms and their influence on the properties of deposition, is the split between in-cloud processes (often involving aerosol emitted/produced at the regional scales or farther) and below-cloud processes which are likely to involve local aerosol. As a result, we find hazardous to speculate further over the available data.

Figure 4: The decimal point is wrong.

We modified the Figure with the correct decimal point

Some new references about urban and remote region pollutants study should be cited in this work, e.g. Dong Z, et al., 2019. Spatial variability, mixing states and composition of various haze particles in atmosphere during winter and summertime in northwest China. Environmental Pollution, 246, (2019) 79-88; 21. Dong Z, et al. Individual particles of cryoconite deposited on the mountain glaciers of the Tibetan Plateau: Insights into chemical composition and sources. Atmospheric Environment, 2016, 138: 114~124. doi: 10.1016/j. atmosenv.2016.05.020

As previously commented, the emission sources and climatological conditions of Moscow megacities have been widely described and motivated by the authors both in the submitted paper and in this letter, with emphasis on soil and road salt resuspension which make up a relevant local contribution to the megacity aerosol.
The atmospheric dynamics behind the processes mentioned in the papers suggested by the estimated reviewer, though appealing, do not apply to our case. Moscow is not a remote area at all, as compared to Tibetan plateau, therefore the relative amount of potentially similar aerosol component is widely different. Moreover, snow cover is not permanent throughout the year; therefore, ground sources of particles become abundantly and promptly available for resuspension and recirculation at the local scale even in weakly energetic conditions. As explained in Lee et al. (2007) Lee, H. N., L. Tositti, X. Zheng, and P. Bonasoni (2007), the Tibetan plateau may be affected by China pollution clouds, but the history and fate of air masses from ground region up to the glacier resume a series of different sources and losses during transport. Analyses and comparisons of variations of7Be, 210Pb, and7Be/210Pb with ozone observations at two Global Atmosphere Watch stations from high mountains, J. Geophys. Res., 112, D05303, doi:10.1029/2006JD007421.1.

Reviewer #2: The authors have revised the manuscript according to the reviewers' comments, and I recommend it to be accepted for publication.

We thank the reviewer for His/Her positive comment